

# A System-Based Comparison of Gene Expression Reveals Alterations in Oxidative Stress, Disruption of Ubiquitin-Proteasome System and Altered Cell Cycle Regulation after Exposure to Cadmium and Methylmercury in Mouse Embryonic Fibroblast

Xiaozhong Yu, Joshua F. Robinson, Jaspreet S. Sidhu,<sup>2</sup> Sungwoo Hong, and Elaine M. Faustman<sup>1</sup>

*Department of Environmental and Occupational Health Sciences, University of Washington, Seattle, Washington, 98105*

<sup>1</sup> To whom correspondence should be addressed at Institute of Risk Analysis and Risk Communication, Department of Environmental and Occupational Health Sciences, University of Washington, 4225 Roosevelt Way NE, Suite #100, Seattle, WA 98105. Fax: (206) 616-4875. E-mail: faustman@u.washington.edu.

<sup>2</sup> Present address: Molecular Epidemiology, Inc., 15300 Bothell Way NE, Lake Forest Park, WA 98155.

Received November 10, 2009; accepted December 28, 2009

Environmental and occupational exposures to heavy metals such as methylmercury (MeHg) and cadmium (Cd) pose significant health risks to humans, including neurotoxicity. The underlying mechanisms of their toxicity, however, remain to be fully characterized. Our previous studies with Cd and MeHg have demonstrated that the perturbation of the ubiquitin-proteasome system (UPS) was associated with metal-induced cytotoxicity and apoptosis. We conducted a microarray-based gene expression analysis to compare metal-altered gene expression patterns with a classical proteasome inhibitor, MG132 (0.5 μM), to determine whether the disruption of the UPS is a critical mechanism of metal-induced toxicity. We treated mouse embryonic fibroblast cells at doses of MeHg (2.5 μM) and Cd (5.0 μM) for 24 h. The doses selected were based on the neutral red-based cell viability assay where initial statistically significant decreases in variability were detected. Following normalization of the array data, we employed multilevel analysis tools to explore the data, including group comparisons, cluster analysis, gene annotations analysis (gene ontology analysis), and pathway analysis using GenMAPP and Ingenuity Pathway Analysis (IPA). Using these integrated approaches, we identified significant gene expression changes across treatments within the UPS (*Uchl1* and *Ube2c*), antioxidant and phase II enzymes (*Gsta2*, *Gsta4*, and *Noq1*), and genes involved in cell cycle regulation pathways (*ccnb1*, *cdc2a*, and *cdc25c*). Furthermore, pathway analysis revealed significant alterations in genes implicated in Parkinson's disease pathogenesis following metal exposure. This study suggests that these pathways play a critical role in the development of adverse effects associated with metal exposures.

**Key Words:** metals; gene expression profiling; ubiquitin-proteasome pathway; cell cycle regulation; oxidative stress.

Environmental and occupational exposures to heavy metals including methylmercury (MeHg) and cadmium (Cd) pose significant health risks to humans and are well-recognized

neurotoxicants (Bergomi *et al.*, 2002; Satarug and Moore, 2004; Verougstraete *et al.*, 2003). Of particular interest is the increasing evidence of a number of neurodegenerative diseases such as Alzheimer's and Parkinson's diseases (PD) for which metal-mediated abnormalities may play a crucial role in disease pathogenesis (Basun *et al.*, 1994; Okuda *et al.*, 1997; Uversky *et al.*, 2001; Weiss *et al.*, 2002). MeHg has been shown to act as a neurotoxicant in humans, nonhuman primates, rodents, and other mammals (Burbacher *et al.*, 1990; Clarkson, 1987). Epidemiologic studies since the 1950's have associated MeHg exposure with a range of neurological effects ranging from mild behavioral alterations to death—dependent on dose, duration of exposure, and age (The National Research Council, 2000). Human exposure is primarily through the consumption of fish and seafood containing accumulated MeHg. Prenatal exposure to MeHg appears to result in a widespread pattern of adverse effects on brain development and organization compared with the relatively restricted brain damage observed when exposure occurs later in life (Burbacher *et al.*, 2005; Choi *et al.*, 1978). Cd is considered to be nephrotoxic and neurotoxic (Chang and Huang, 1996) and has been classified as a human carcinogen by International Agency for Research on Cancer (2009). It is a ubiquitous contaminant, entering the environment through a number of sources, including batteries, pigments, plastics, mining, smelting, and cigarette smoke (Beyersmann and Hechtenberg, 1997). Ingestion is the main route of entry for the nonsmoking population with exposures averaging 1.4–25 μg/day (Elinder *et al.*, 1985). Cadmium has an extensive biological half-life (> 20 years) and can exhibit toxic insult on numerous tissues, including the central nervous system (Goering *et al.*, 2000).

Despite extensive research conducted over the last half century, the molecular mechanisms underlying the observed adverse effects of heavy metals such as MeHg and Cd are still

fragmental. Previous studies using a variety of experimental systems have shown that metals affect multiple intracellular targets and exert various effects on cells *in vitro* (Castoldi *et al.*, 2003; Fonnum and Lock, 2004; Philbert *et al.*, 2000). These metal effects are a result of both common and unique mechanisms that are cell or tissue specific (Ercal *et al.*, 2001; Figueiredo-Pereira *et al.*, 2002; Sarafian, 1999). MeHg and Cd toxicity have been associated with oxidative stress, altered cell cycle regulation, and apoptosis (Bertin and Averbeck, 2006; Gribble *et al.*, 2005; Robinson *et al.*, 2009; Yu *et al.*, 2008a). Interestingly, the ubiquitin-proteasome system (UPS) has been postulated to be associated with the cellular response to heavy metal exposure (Figueiredo-Pereira *et al.*, 1998; Kirkpatrick *et al.*, 2003; Stewart *et al.*, 2003). The UPS is a highly conserved cellular pathway that plays an important role in the selective degradation of cellular proteins that are essential for the regulation of a variety of vital cellular functions (Hershko and Ciechanover, 1998; Joazeiro and Hunter, 2000). Disruption of this posttranslational system, therefore, can have significant downstream effects on critical cellular functions, impacting susceptibility and development of disease. MeHg and Cd have shown that the perturbation of the UPS is important in mediating metal-induced cytotoxicity and apoptosis (Hwang *et al.*, 2002; Jungmann *et al.*, 1993; Tsigotis *et al.*, 2001; Yu *et al.*, 2008a). The progressive accumulation of ubiquitinated protein conjugates has been associated with pathologic observations within humans, including brain aging and neurodegenerative diseases (De Vrij *et al.*, 2001; Forloni *et al.*, 2002; Iseki *et al.*, 1996; Lam *et al.*, 2000). The objective of our study, therefore, was to clarify the role of the UPS in cellular response to heavy metals and to identify the critical pathways that might influence susceptibility to the development of neurodegenerative diseases.

The integration of genome-wide array data with knowledge-based pathway mapping facilitates the elucidation of the underlying molecular mechanisms of metal-induced toxicity. In this paper, comparisons based on microarray analysis across the two metals and the classical proteasome inhibitor MG132 (0.5  $\mu$ M) have facilitated the delineation of important molecular events that are mechanistically linked with observed functional or toxic end points. This has allowed us to test whether the disruption of the UPS is a critical mechanism of metal-induced toxicity. We have applied mouse embryonic fibroblast (MEF) cells as our model to define molecular events involved in metal-mediated neurodegeneration at relevant low doses of MeHg (2.5  $\mu$ M) and Cd (5.0  $\mu$ M) for 24 h. MEFs are an ideal model system for studying aspects of cell growth control and functional genetics because of the ability to derive these cells from mice harboring various genetic alterations in addition to the ease with which isolation of MEF from mid-gestation mouse embryos is made (Lowe *et al.*, 1994; Sharpless *et al.*, 2004; Steinman *et al.*, 2004). MEFs have also widely been used as valuable cell culture models to examine signaling pathway changes under varying conditions (Ramana *et al.*,

2005; Vengellur *et al.*, 2003). Unlike immortal and transformed cell lines, MEFs retain their initial growth characteristics and genetic backgrounds, assuring more biologically relevant results. We have applied this culture system to investigate the molecular mechanisms of metal-induced cell cycle arrest, apoptosis, as well as the role of p53 (Gribble *et al.*, 2003, 2005; Sidhu *et al.*, 2003; Yu *et al.*, 2008b). Using an integrated systems-based approach, we identified significant alterations in the UPS, antioxidant and phase II enzymes, as well as in the genes involved in the regulation of the cell cycle. Further pathway analysis revealed significant alterations in genes implicated in the pathogenesis of PD, especially for Cd. This study emphasizes the critical role of the above pathways and the resulting harmful effects of metal exposure.

## MATERIALS AND METHODS

**Cell culture.** MEFs were obtained following a modified protocol (Gribble *et al.*, 2005). Embryos were separated from the uteri of 14-day-old pregnant female mice (C57BL/6) and were washed several times in Earl's Balanced Salt Solution (Gibco BRL, Grand Island, NY). The torso and limbs were then dissected in order to isolate the fibroblasts. Single-cell suspensions were plated in 100-mm dishes in Dulbecco's Modified Eagle Medium: nutrient mixture F-12 with 10% vol/vol Nu-Serum, 2mM L-glutamine, 100 U/ml penicillin, and 100  $\mu$ g/ml streptomycin—all obtained from Gibco BRL. Cells were kept in a humidified 37°C incubator with 5% CO<sub>2</sub>.

**Metal treatment, cell cytotoxicity, and cell cycle alterations.** MEFs at passage 6 or 7 were grown to near confluency (85–90%) and then synchronized by reducing Nu-serum concentration to 0.05% for 24 h in a humidified atmosphere of 5% CO<sub>2</sub>/95% air at 37°C. MEF cells were treated with methylmercury (II) hydroxide (MeHg, 0–4  $\mu$ M), cadmium chloride (Cd, 0–20  $\mu$ M), as well as MG132 (0.05–2.5  $\mu$ M) for 24 h. All applications of MeHg and Cd were conducted in a Class II type B2 hood (Biochemguard; The Baker Company Inc., Sanford, ME). The cultures were monitored with an inverted phase-contrast microscope to assess their general appearance (Yu *et al.*, 2005). Cell viability was determined using the neutral red (NR) uptake assay based on lysosomal accumulation of NR in viable cells. Cells were harvested, and total protein and messenger RNA (mRNA) were extracted, as described previously (Yu *et al.*, 2005). Cell cycle kinetics were examined using bivariate BrdU-Hoechst flow cytometry—according to our established protocol—and allows for the dynamic change of cell cycle progression to be monitored (Sidhu *et al.*, 2005). Cells were cultured with 5-bromo-2'-deoxyuridine (BrdU) to incorporate BrdU into their DNA. After incubation, cells were harvested and resuspended in Hoechst 33258 buffer and propidium iodide (PI) with RNase (0.1%). Cells were analyzed using a Coulter Epics Elite flow cytometer (Beckman Coulter). MPLUS 5.0 software (Phoenix Flow Systems) was used to analyze the data. Analysis was conducted to determine the proportion of cells in each cell cycle phase (G<sub>0</sub>/G<sub>1</sub>, S, and G<sub>2</sub>/M) from successive rounds of cell division.

**RNA isolation and microarray hybridization.** Cells in 100-mm plates were rinsed twice with ice-cold calcium and magnesium free-PBS and lysed with 1 ml Trizol (Invitrogen, San Diego, CA) 24 h after treatment. Three independent samples were collected per treatment. The total RNA isolations were conducted according to the recommended protocol (Invitrogen). Total RNA was further purified by using the RNeasy Mini Kit (Qiagen, Valencia, CA). Quality of the RNA was assessed on the Agilent 2100 Bioanalyzer (Agilent, Palo Alto, CA) running the RNA 6000 assay. A 500-ng aliquot of each sample was loaded in order to measure 18S and 28S ribosomal RNA (rRNA). A profile for intact RNA yielded near to a 2 to 1 ratio of 28S rRNA to 18S rRNA.

Microarray analysis was conducted in the University of Washington's Functional Genomics Laboratory—Center for Ecogenetics and Environmental Health, following the manufacturer's protocols for the technical aspects associated with the determination of gene expression using the Amersham "CodeLink" platform. The first step in preparing samples for hybridization was the synthesis of complementary DNA (cDNA) from 5 µg of RNA using Superscript II. Using 0.5 pmol of T7-(dT)<sub>24</sub> primer, the RNA was denatured for 10 min at 70°C and then incubated for 1 h at 42°C with reverse transcription. Following first-strand synthesis, double-stranded cDNA was generated with the addition of *Escherichia coli* DNA polymerase. Next, the RNA template was degraded with RNase H during a 2-h incubation at 16°C. The resulting cDNA column was purified using the QIAquick purification kit for PCR products (Qiagen). Finally, complementary RNA (cRNA) was produced from the second strand of DNA using the In Vitro Transcription Kit (Amersham Biosciences, Piscataway, NJ). In addition to the nucleotide mix, 10 µl Biotin-11-UTP was added (Perkin Elmer Life Sciences, Boston, MA). After 14 h at 37°C, the reaction was stopped and the amplified product column was purified with the RNeasy Mini Kit (Qiagen). The cRNA was measured by testing its absorbance at 260 nm on an ultraviolet spectrophotometer. The quality of the cRNA was assessed on the Agilent 2100 Bioanalyzer. The RNA profile of a successful cRNA synthesis resembled a smear from 250 to 5500 nt, with a peak between 1000 and 1500 nt. Next, the cRNA was stored at -80°C until it was used for array hybridization. No more than 10 µg of biotinylated cRNA was fragmented at 94°C for 20 min. Two hundred and fifty microliters of the fragmented label in buffer solution was loaded into each slide chamber. Hybridization was carried out for 18 h at 37°C on an orbital shaker set to 300 rpm. After they were removed from the hybridization chamber, the arrays were washed with 0.75 × 0.1 M Tris-HCl, pH 7.5, 0.15 M NaCl, and 0.05% Tween 20 (TNT) for 1 h at 46°C. A 30-min incubation period with AlexaFlour 647-streptavidin (Molecular Probes, Inc., Eugene, OR) was followed by four 5-min washes in 1 × TNT and two vigorous rinses in 0.05% Tween-20. The slides were dried by centrifugation at 350 × g for 3 min. Once dried, the arrays were scanned on an Axon GenePix 4000 Scanner (Axon Instruments, Union City, CA) and set to a wavelength of 635 nm with a photomultiplier voltage of 600 V and a 10µm resolution.

**Statistical analysis and comparisons.** CodeLink array data were first run through the accompanying software from Amersham Biosciences. The array data were deposited NCBI gene expression omnibus (<https://www.ncbi.nlm.nih.gov/geo/query/browse.cgi>). In order to complete the statistical analysis, the raw data were input to the BRB Array Tools (Wright and Simon, 2003). A log<sub>2</sub> transformation was applied to the data and normalized for each array by using its median intensity. A class comparison was conducted in each treatment by using the randomized variance model. Because standard *t/F*-test variance estimates are not accurate and their statistical power is poor, the randomized variance *t*- and *F*-tests were found to be a better alternative when there were fewer samples ( $n = 2-5$ ) in each class (Long *et al.*, 2001; Wright and Simon, 2003). Nonsupervised two-dimensional hierarchical clustering was performed as follows: The significantly changed genes (1754 genes) among the four groups were selected based on a multivariate permutations test (1000 random permutations). The nominal significance level of each univariate test was  $p \leq 0.001$ , and the confidence level of false discovery rate assessment was 90%. The maximum allowed number of false-positive genes and maximum allowed proportion of false-positive genes were 10 and 0.1, respectively. The significant genes were further filtered and the geometric mean intensity varied more than fourfold over the control (both directions) in at least one of the treatment groups. For the selected genes (497), ratios were derived by dividing each normalized gene value with the average value of the controls and were then transformed to a log<sub>2</sub> ratio. A hierarchical clustering analysis on the output genes using average linkage and Euclidean dissimilarity was conducted using the log<sub>2</sub>-transformed ratio input to the MultiExperiment Viewer (MEV) (Eisen *et al.*, 1998; Saeed *et al.*, 2003). The complete output of cluster analysis is shown with the fold change, indicated colorimetrically.

**A systems-based functional gene ontology and pathway analysis of microarray data.** Functional microarray analysis was conducted based on our recently established gene ontology (GO)-quant approach (Yu *et al.*, 2006,

2008b, 2009). We identified enriched biological themes, particularly GO terms at  $p \leq 0.001$ , by applying the MAPFinder. This enabled us to establish the association between the treatment and the affected GO terms (Doniger *et al.*, 2003). A Z-score and permutation *p* value were used to rank the biological significance of these terms. MAPFinder calculates the percentage of the genes that are significantly upregulated (fold  $\geq 1.5$  and  $p < 0.05$ ) or downregulated (fold  $\leq 0.67$  and  $p < 0.05$ ). Z-scores, the statistical measure of significance for gene expression in a given group, were calculated by subtracting the number of genes expected to be randomly changed in a GO term from the observed number of changed genes in that GO term. A permutations test for the Z-score, based on a nonparametric bootstrapping approach, was calculated to address the multiple testing. For a GO term (GOID) to be included in the table, at least five genes needed to be significantly changed and the permutation *p* value needed to be  $\leq 0.01$ . Signal pathways, especially antioxidant and detoxification enzyme and cell cycle regulation pathways, were evaluated for differential regulation using the visualization tool GenMAPP (Doniger *et al.*, 2003; Yu *et al.*, 2008b, 2009).

Next, a canonical pathway-based analysis was conducted using the IPA (Ingenuity Systems, [www.ingenuity.com](http://www.ingenuity.com)) for each treatment in order to identify the genes associated with canonical pathways in the Ingenuity Pathways Knowledge Base. Genes from the each treatment that met the significance *p* value cutoff of 0.01 and fold change cutoff of 1.5 were associated with a canonical pathway in Ingenuity's Knowledge Base and were considered for the analysis. The significance of the association between the each treatment and the canonical pathway was measured in two steps. First, the ratio of the number of genes from each treatment that map to the pathway, divided by the total number of genes that map to the canonical pathway, was calculated. Second, a Fisher's exact test was used to calculate a *p* value determining that the probability of the association between the genes in each treatment and the canonical pathway was random.

**Validation of gene expression from microarray by quantitative real-time PCR.** Validation of alterations in gene expression induced by metals and MG132 determined by microarray was conducted using a fluorogenic 5' nuclease-based assay and quantitative real-time-PCR (qRT-PCR) (Diaz *et al.*, 2001; Lin *et al.*, 2002; Yu *et al.*, 2008b). MEFs were treated with Cd (5µM), MeHg (2.5µM), and MG132 (0.5µM) under the same conditions used in the microarray study. Three biological samples were included in each treatment. Cells were harvested 4, 8, and 24 h after each treatment. RNA was collected and purified as mentioned above. A cDNA synthesis was generated using Oligo(dT)<sub>12-18</sub> and Superscript II Reverse Transcriptase (Gibco BRL). A qRT-PCR analysis was conducted using SYBR Green (Applied Biosystems, Inc., Foster City, CA) for Gsta2 from the antioxidant and phase II enzyme pathway, TaqMan (Applied Biosystems) for Uchl1 and Ube2c involved in the UPS pathway, Ccnb1 and Cdc25c from the cell cycle pathway, and, lastly, Snca from the PD pathway. To induce gene expression for the genes Ccnb1, Cdc25c, Uchl1, Ube2c, Snca, and GAPDH, 4 µl of cDNA was included in a PCR (25 µl final volume). The reaction also included the appropriate forward and reverse primers at 360nM each, 80nM TaqMan probe, 1 × TaqMan Universal PCR Master Mix, and No Amperase UNG (Applied Biosystems Inc.). The PCR for Gsta2, on the other hand, consisted of 120nM of each primer and 1 × SYBR green PCR Master Mix (Applied Biosystems Inc.). The PCR primers and the dual-labeled probes (6-carboxy-fluorescein [FAM] and 6-carboxy-tetramethyl-rhodamine [TAMRA]) for all genes were designed using ABI Primer Express v.1.5 software (Applied Biosystems Inc.). The oligo sequences are listed in Table 1. Amplification and detection of PCR amplicons were performed with the ABI PRISM 7700 system (Applied Biosystems Inc.) with the following PCR profile: 1 cycle of 95°C for 10 min, 40 cycles of 95°C for 30 s and 62°C for 1 min. GAPDH amplification plots derived from serial dilutions of an established reference sample (mouse liver RNA) were used to create a linear regression formula in order to calculate Ccnb1, Cdc25c, Uchl1, Ube2c, Snca, and Gsta2 expression levels. GAPDH gene expression levels were utilized as internal controls to normalize the data. Reported fold changes in expression are the ratios of treatment over control values. A correlation of the gene expression of five selected genes (in log<sub>2</sub> fold) between the

**TABLE 1**  
**Sequences for PCR Primers and Probes**

Gene	Forward primer (FOR) Reverse primer (REV)	Probe
Cyclin B1	FOR: 5'-TGAAGACTCCCTGCTTCCTGTTATG-3' REV: 5'-TCAGCTGTGCCAGCGTGC-3'	5'-FAM-TCACAAAGCACATGACTGTCAAGAACAAGTATGC A-TAMRA-3'
Cdc25c	FOR: 5'-GCATTATATTACCCTGAGCTATATATCCTCAA-3' REV: 5'-GAAGCATGGGACAGTAGCTCTGTG-3'	5'-FAM-TCACACAGCTCCATATACTCTGGAAAGAAATCTC TGTAGC-TAMRA-3'
Uchl1	FOR: 5'-TGCCCTTCCAGTGAACCATG-3' REV: 5'-CAGAGAAGCGGACCTCCCC-3'	5'-FAM-TGGCAGCATCTCTGCAGCAGAGAGTCC-TAMRA-3'
Ube2c	FOR: 5'-TCTATCCAGAGCCTGCTAGGAGAAC-3' REV: 5'-CTTGCTGGAGACCTGCTTTG-3'	5'-FAM-AAAACCCACAGCATTAAAGAAATACCTGCAAGA AAC-TAMRA-3'
Snca	FOR: 5'-GGATCTGGCAGTGAGGCTTA-3' REV: 5'-GCAGATCTTAGGAGATTGGGTGC-3'	5'-FAM-CCTTCAGAGGAAGGCTACCAAGACTATGAGCCTG- TAMRA-3'
Gapdh	FOR: 5'-TCCTGCACCACCAACTGCTT-3' REV: 5'-GAGGGCCATCCACAGTCTT-3'	5'-FAM-CACTCATGACCACAGTCCATGCCATCAC-TAMRA-3'
Gsta2	FOR: 5'-GTATTATGTCCCCAGACCAAAGAG-3' REV: 5'-CTGTTGCCACAAGGTAGTCTTGT-3'	

microarray and qRT-PCR was performed in JMP (JMP for Windows V 5.0; SAS Institute, Cary, NC).

## RESULTS

### *Cytotoxicity and Cell Cycle Alteration Induced by Cd, MeHg, and MG132*

In this study, we examined metal-induced morphological alterations, cytotoxicity, and cell cycle arrest. MG132, MeHg, and Cd<sup>2+</sup> induced a dose-dependent cytotoxicity as seen by the disruption of cellular morphology (Figs. 1A–D) and attenuated cell viability using the NR uptake assay (Figs. 1E–G). As shown in Figures 1A–D, increases of irregular cell shape and dead cells became obvious in the treatment with MG132 at 0.5µM, MeHg at 2.5µM, and Cd at 5µM for 24 h. Decreases in cell viabilities were initially observed at concentrations of 0.5µM with MG132 treatment, 2.5µM with MeHg treatment, and 5µM with Cd treatment.

MG132 treatment at 0.5µM resulted in significant accumulation of cells in G<sub>2</sub>/M phase (24 and 48 h) (Fig. 2A) and a decrease of cells in the new G<sub>0</sub>/G<sub>1</sub> phase (Fig. 2B). In the MeHg-treated cells, a significant increase of the cell population in G<sub>2</sub>/M phase was observed at concentrations of ≥ 1µM (Fig. 2A) and less cell progressing to the new G<sub>0</sub>/G<sub>1</sub> at concentrations of ≥ 1µM at 24 h and 2.5µM at 48 h (Fig. 2B). Cd treatment resulted in a dose-dependent inhibition of cell cycling that was observed as an increase in the cell population in G<sub>2</sub>/M phase (Fig. 2A) and a decrease in cells taking up BrdU (new cell cycle G<sub>0</sub>/G<sub>1</sub>) at concentrations of ≥ 2.5µM (24 and 48 h) (Fig. 2B).

### *Gene Expression Response to MG132*

A total of 426 genes were found to be responsive to MG132, our model protease inhibitor at the cutoff of  $p \leq 0.001$

(randomized *t*-test). Among them, 166 genes were significantly upregulated, while 260 genes were significantly downregulated (Fig. 3A). As shown in Figure 3A, the top 10 upregulated genes (fold > 5) were P2rx11, Cpxm1, Agrp, Mocos, Gsta3, Dncic1, Uchl1, Gsta2, Gsta4, and Ppl. The top 10 down-regulated genes (fold < 0.18) were cell cycle regulatory genes, such as 2010317E24Rik, Il1a, Kif20a, Tk1, DNA D2Erd750e, Ube2c, 2600017J23Rik, Kif4, Cdca3, and Hp.

We used MAPPFinder to find significant changes by gene functional category. MAPPFinder linked 9996 probe sets measured in this experiment to the GO database. The 7721 probe sets were linked to GO terms in the hierarchy and then the percentage of genes meeting the criteria of either a significant increase (fold ≥ 1.5 and  $p \leq 0.05$ ) or decrease (fold ≤ 0.67 and  $p \leq 0.05$ ) in fold change expression was calculated. Following this, a Z-score for each GO term was assigned. MAPPFinder results represent a global picture of biological processes, cellular components, and molecular functions (Table 2) that are significantly altered at the transcriptional level in MEFs after 24 h with MG132 treatment (at least five genes needed to be significantly changed and the permutation  $p$  value ≤ 0.01).

Catabolism (GOID 9056), especially UPS-dependent protein catabolism as shown in Supplementary table 1A, was significantly upregulated (GOID 6508, 19941, and 6511). Coenzyme metabolism (GOID 6731, 46138, and 6732), nucleotide metabolism (GOID 9117, 9141, 9142, 9145, 9206, 6754, 9201, 9144, 9205, 46034, 9199, 6164, 9152, 9260, 6163, 9150, and 9259), carbohydrate metabolism (GOID 5975), glutathione (GSH) metabolism (GOID 6749), and sulfur metabolism (GOID 6790) were also upregulated (Table 2).

MG132 induced the upregulation of the molecular functions of GSH transferase activity (GOID 4364), hydrolase activity (GOID 16787, 16820, 42626, 8553, 16789, 4553, and 4553), and peptidase activity (GOID 8233), including endopeptidase

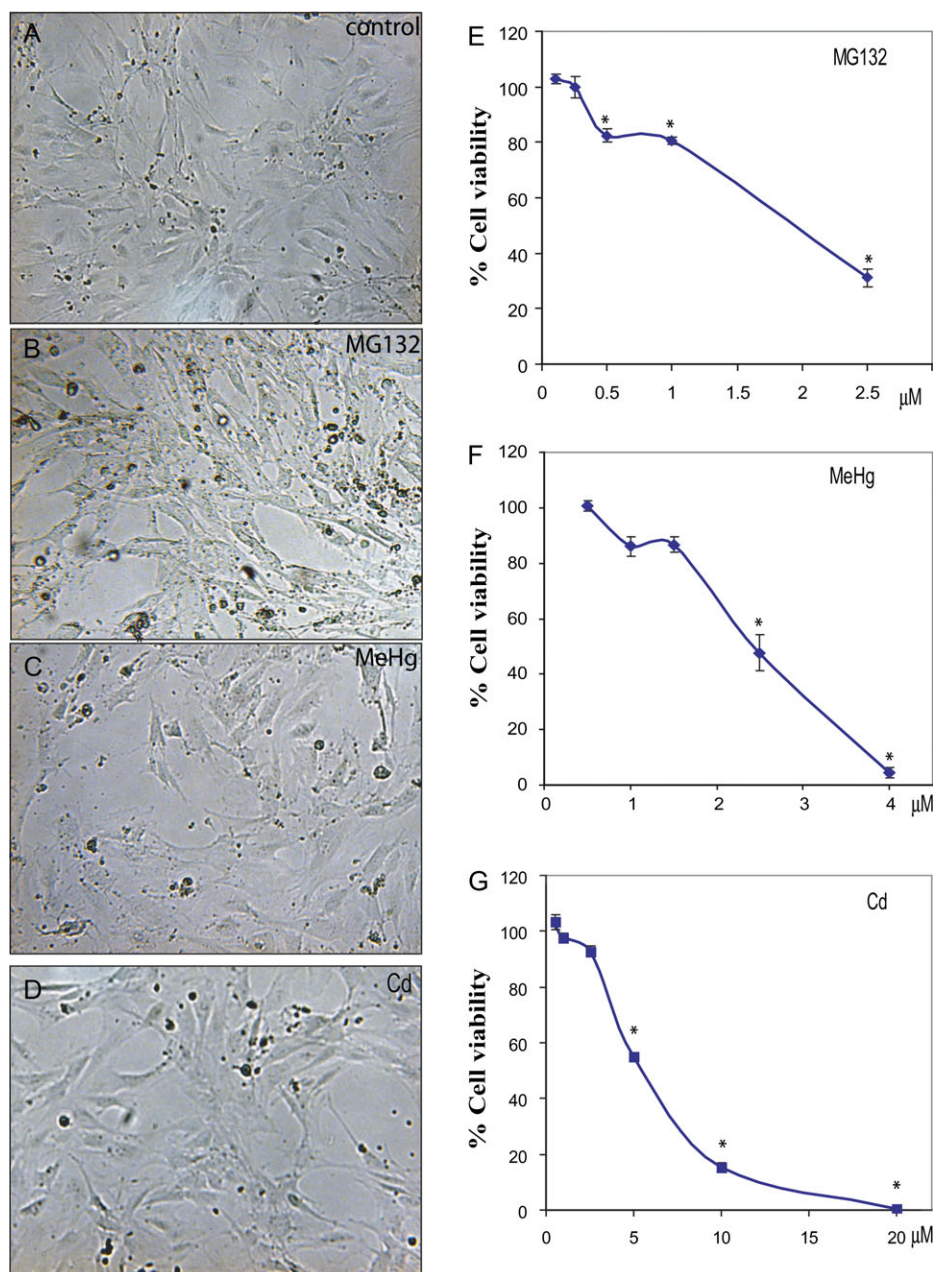


**FIG. 1.** Morphology changes (A–D) and cell viability (E–G) induced by MG132, methylmercury (MeHg), and cadmium (Cd) in MEF cells. Cultures of MEF cells were exposed to various concentrations of Cd, MeHg, and MG132 for 24 h. Following exposure, cell morphological changes were monitored with an inverted phase-contrast microscope. Typical photos for the control (A), MG132 (0.5 μM, B), MeHg (2.5 μM, C), and Cd (5 μM, D) for 24 h were listed. Cell viability was assessed utilizing the NR uptake assay, which reflects the uptake function of the cells (E–G). Statistical analysis of cell viability was conducted using one-way ANOVA ( $p \leq 0.05$ ), followed by Dunnett's method to the control, with a significance level of  $p \leq 0.05$  (\*). Data are presented as mean  $\pm$  SE,  $n \geq 3$ .

(GOID 4175), exopeptidase (GOID 8238), and metallopeptidase (GOID 8237). The most significant cellular components to be upregulated were the proteasome complex (GOID 502 and 5839), lysosome (GOID 6764, 323, and 5773), microtubule (GOID 15630 and 5875), and endoplasmic reticulum (GOID 5783) (Supplementary table 1A).

As shown in Supplementary table 1B, MG132 significantly downregulated genes involved in cell proliferation (GOID

8283). This is demonstrated in the downregulation of genes associated with cell cycle regulation, including M phase (GOID 279, 87, 7067, 280, and 278), S phase (GOID 84), cell cycle checkpoint (GOID 75), regulation of cell cycle (GOID 74 and 45786), and DNA replication (GOID 67, 7059, 6260, 6261, and 6270). DNA metabolism such as DNA packaging (GOID 6323), recombination (GOID 6310), repair (GOID 6281), and nuclear organization (GOID 6997, 7001, 6333, and 63334)

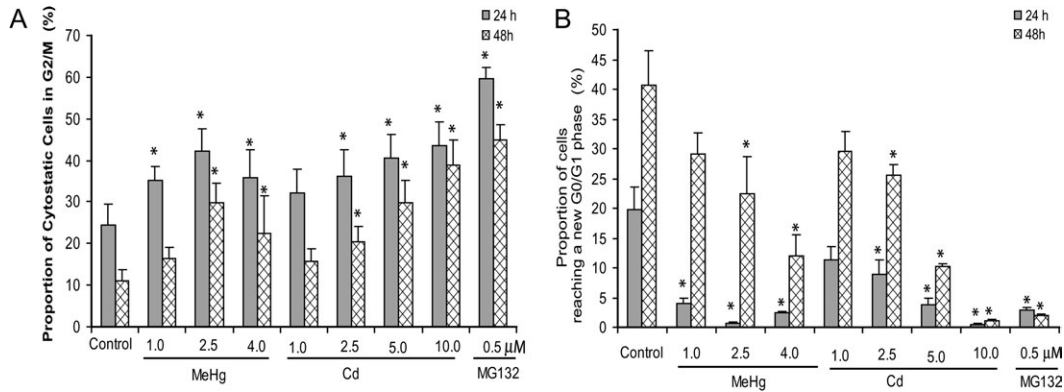


**FIG. 2.** Cell cycle alterations by MG132, methylmercury (MeHg), and cadmium (Cd) in MEF cells. Cultures of MEF cells were exposed to various concentrations of Cd, MeHg, and MG132 for 24 h. Evaluation of bivariate Hoechst-PI flow cytograms was conducted to determine the total number of cells and the proportion of cells in the first and successive rounds of cell division. Statistical analysis was conducted using ANOVA, followed by Dunnett’s method to the control, with a significance level of  $p \leq 0.05$  (\*). Data are presented as mean  $\pm$  SE,  $n \geq 3$ . Dose-dependent increases in proportion of cytotostatic cells in G<sub>2</sub>/M (A) and decreases in proportion of cells into new G<sub>0</sub>/G<sub>1</sub> (B) phase were observed.

were also significantly downregulated. Response to DNA damaging (GOID 6974) and stress (GOID 6950) were upregulated.

MG132 significantly downregulated genes in DNA-dependent ATPase activity (GOID 8094 and 3887), enzyme regulatory activity (GOID 30234) such as protein kinase regulatory activity (GOID 19887, 16538, and 19207), trans-ferase activity (GOID 16740, 16772, 16779, and 3887), as well as G-protein-coupled receptor binding (GOID 1664), such as chemokine activities (GOID 8009). Significantly downregulated genes in the cellular components were observed in chromosome (GOID 5694), replisome (GOID 30894), replica-

tion fork (GOID 5657), and spindle (GOID 5819 and 922). The above changes in the cellular component were consistent with the downregulation in cell proliferation, especially in the cell cycle of the biological process.

*Gene Expression Response to MeHg*

MeHg treatment altered a total of 744 genes,  $p \leq 0.001$  (Fig. 3B). Of these genes, 294 were significantly upregulated in expression and 450 were downregulated (Fig. 3B). Figure 3B shows the most significantly upregulated genes. These include glutathione S-transferase Gsta2 and Gsta3, Arg2, Igh-6, 1700012B18Rik, Mmp10, Serpinb2, Akr1c18, Mmp13, and

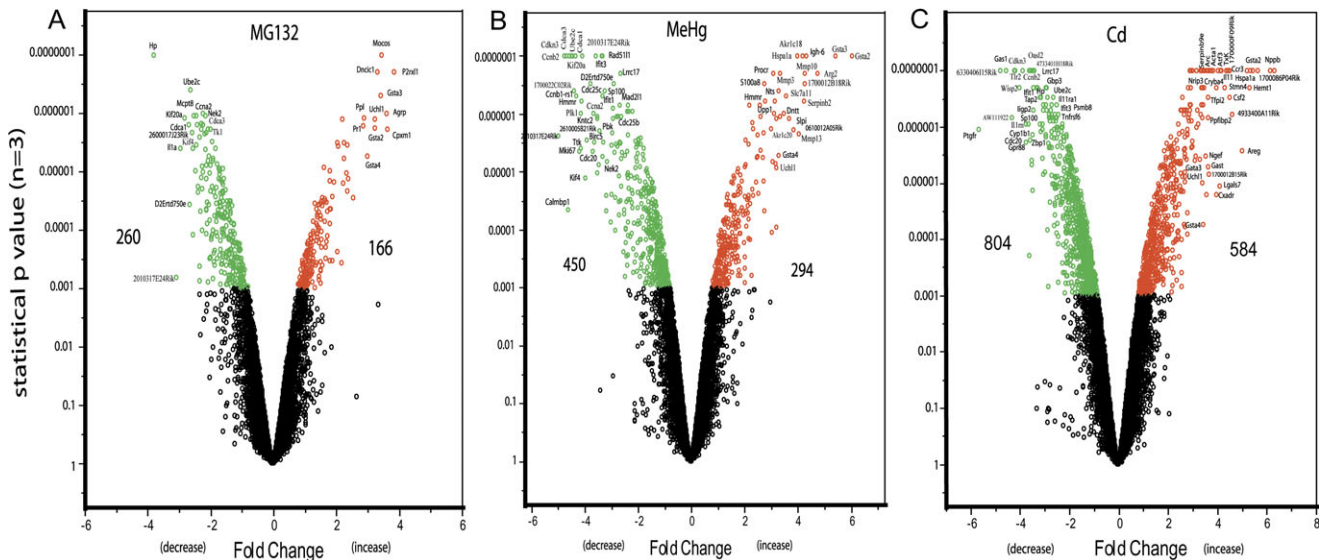


**FIG. 3.** Volcano plot showing gene expression alteration after exposure to MG132 (A), methylmercury (MeHg, B), and cadmium (Cd, C) in MEF cells. Cultures of MEF cells were exposed to Cd (5 $\mu$ M), MeHg (2.5 $\mu$ M), and MG132 (0.5 $\mu$ M) for 24 h. A microarray-based gene expression analysis was conducted as described in the “Materials and Methods” section. A randomized variance *t*-test (Wright and Simon, 2003) was used to select the significant downregulated genes (green) and upregulated genes (red) at  $p \leq 0.001$  ( $n = 3$ ). The x-axis of the figure is the base 2 logarithm of the fold change over the control ( $n = 3$ ). The y-axis is negative base 10 logarithm of the  $p$  value for the per gene *t*-test.

TABLE 2

Comparison of Gene Expression Results between the Codelink Microarray and qRT-PCR in MEFs Exposed to MG132, Methylmercury (MeHg), and Cadmium (Cd) for 24 h. qRT-PCR Gene Expression Measurements for GST2a, Uchl1, Ube2c, Ccnb1, Snca, and Cdc25c in Three Biological Samples Exposed Under the Same Conditions as Microarray Studies were Evaluated as Described in the "Materials and Methods" section. Data are Presented as Mean  $\pm$  SE,  $n = 3$

	Gene	Gsta2	Uchl1	SNCA	Ube2c	Ccnb1	Cdc25c
Cd	Codelink	43.65 $\pm$ 5.03	5.23 $\pm$ 0.60	5.31 $\pm$ 0.43	0.14 $\pm$ 0.03	0.18 $\pm$ 0.09	0.20 $\pm$ 0.06
	qRT-PCR	40.94 $\pm$ 8.93	2.02 $\pm$ 0.07	14.65 $\pm$ 5.84	0.25 $\pm$ 0.03	0.57 $\pm$ 0.01	1.28 $\pm$ 0.09
MG132	Codelink	9.50 $\pm$ 0.93	9.53 $\pm$ 1.35	0.95 $\pm$ 0.08	0.16 $\pm$ 0.01	0.19 $\pm$ 0.01	0.21 $\pm$ 0.01
	qRT-PCR	26.25 $\pm$ 1.58	12.89 $\pm$ 0.57	5.09 $\pm$ 1.68	0.02 $\pm$ 0.01	0.03 $\pm$ 6.27	0.80 $\pm$ 0.14
MeHg	Codelink	64.16 $\pm$ 19.60	9.20 $\pm$ 3.60	0.68 $\pm$ 0.06	0.05 $\pm$ 0.01	0.05 $\pm$ 0.02	0.10 $\pm$ 0.01
	qRT-PCR	36.54 $\pm$ 4.04	11.77 $\pm$ 0.43	0.24 $\pm$ 0.13	0.25 $\pm$ 0.03	0.58 $\pm$ 0.08	0.38 $\pm$ 0.13

Hspa1a. The top 10 downregulated genes in magnitude were 2010317E24Rik, Ccnb2, Cdkn3, Calmbp1, Cdca3, Cdca1, Ube2c, 1700022C02Rik, 2600017J23Rik, and Ccnb1.

Using MAPPFinder (Supplementary table 2A), we found MeHg upregulated a number of biological process genes especially in the regulation of protein kinase activity (GOID 45859, 6469, 7243, and 165); GSH metabolism (GOID 6749); the modification of dependent protein catabolism, such as ubiquitin-dependent protein catabolism (GOID 19941 and 6511); immune and inflammatory response (GOID 45087 and 6954); response to heat and stress (GOID 9266, 9408, and 6950); and lastly, in cell death (GOID 8219) (Supplementary table 2A). In the cellular component category, proteasome complex genes (GOID 5839) were the only significantly upregulated category (Supplementary table 2A). This is consistent with the activation of UPS-dependent protein degradation as observed in the biological process. In the molecular functional gene category, MeHg upregulated protein tyrosine activity (GOID 8138) and chaperone activity genes (GOID 3754), such as heat-shock protein (HSP) activity (GOID 3773) (Supplementary table 2A).

MeHg treatment downregulated genes in the cell proliferation (GOID 8283) as exhibited in the downregulation of cell cycle genes (Supplementary table 2B). Genes in DNA replication (GOID 67, 7059, 6260, and 6261), M phase (GOID 279, 87, 7067, 280, and 278), S phase (GOID 84), and cytokinesis (GOID 910); DNA metabolism (GOID 6259) such as DNA repair (GOID 6281); and responses to stimulus especially to DNA damage stimulus (GOID 6974 and 9719) were also downregulated in MeHg exposure. In the molecular function category, MeHg significantly downregulated genes in the extracellular matrix structural constituent (GOID 5201 and 30020); oxidoreductase activity (GOID 16491, 16705, and 16706); protein kinase activity, such as cyclin-dependent protein kinase regulators (GOID 16301, 4672, 4674, 19207, 19887, and 16538); and catalytic activity (GOID 3824, 4527, 8408, and 8081) (Supplementary table 2B). In the cellular component, MeHg downregulated genes in the chromosome (GOID 5694), such as replisome and replication fork (GOID

775, 5657, and 30894), and Spindle (GOID 5819 and 922). The above genes are involved in cell cycle progression. Other genes in the extracellular matrix (GOID 5578 and 5581), cell-matrix junction (GOID 30055, 5924, and 5925), and microtubule cytoskeleton (GOID 5815) were also significantly downregulated (Supplementary table 2B).

#### Gene Expression Response to Cd

A total of 1388 genes were observed to be altered after Cd treatment,  $p \leq 0.001$  (Fig. 3C). Among them, 584 genes were significantly upregulated and 804 genes were downregulated. As shown in the Figure 1B, the most significantly upregulated genes (mean fold > 20) were Serpinb2, 2210011C24Rik, Nppb, Gsta2, Hspa1a, Hemt1, 1700086P04Rik, Areg, 4933400A11Rik, and Csf2. The top downregulated genes (fold < 0.05) were Ptgfr, 6330406I15Rik, Gas1, AW111922, Cdkn3, Oasl2, Wisp2, Tlr2, Ccnb2, and Il1m.

MAPPFinder results linking gene expression data of Cd exposure to the GO database are shown in Supplementary table 3A and B. In the biological process category, Cd upregulated a variety of gene categories, including response to stimulus, stress and heat (GOID 9605, 9628, 9266, 9408, and 6950), regulation of protein kinase activity (GOID 45859 and 6469); transport (GOID 15837, 15849, 46942, and 6865); and ubiquitin-dependent protein catabolism (GOID 6511 and 19941). In the molecular category (Supplementary table 3A), chaperone activity (GOID 3754) such as HSP activity (GOID 3773) and a variety of transporter activity (GOID 5275, 15171, 5279, 15203, 5342, and 46943) were upregulated (Supplementary table 3A). In the cellular component category, genes in intermediate filament (GOID 45111 and 5882) were upregulated.

A significant decrease in cell proliferation with Cd treatment was observed (GOID 8283) (Supplementary table 3B). There was significant downregulation in cell cycle genes (GOID 7049), associated with the M phase (GOID 279, 87, 7067, 280, and 278), and cytokinesis (GOID 910) (Supplementary table 3B). DNA metabolism (GOID 6259) such as DNA-packaging genes (GOID 6323) and repair genes

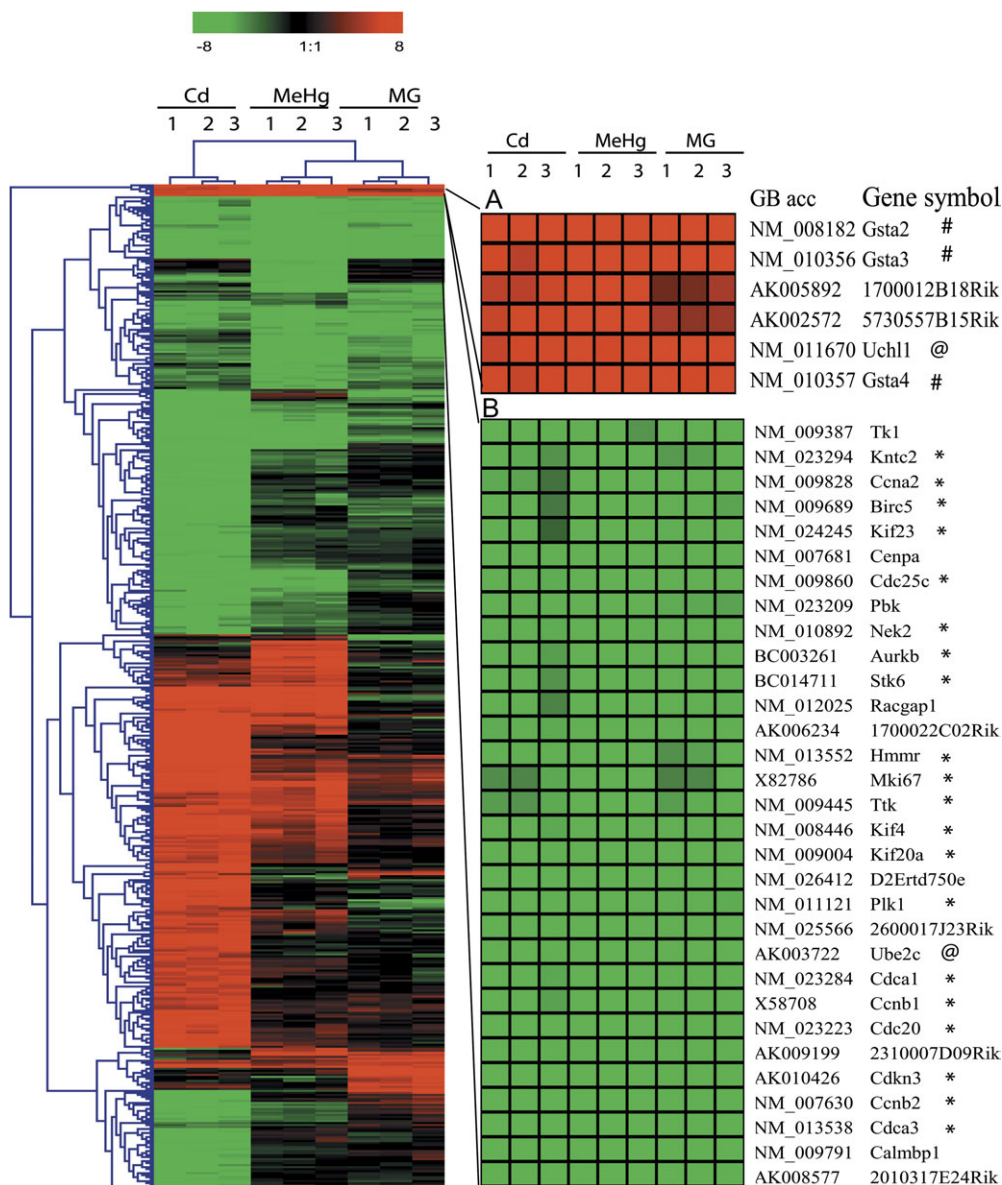


**FIG. 4.** Hierarchical cluster analysis of differentially expressed genes in MEF cells exposed to MG132, methylmercury (MeHg), and cadmium (Cd). Cultures of MEF cells were exposed to Cd (5µM), MeHg (2.5µM), and MG132 (0.5µM) for 24 h. A microarray-based gene expression analysis was conducted as described in the “Materials and Methods” section. A randomized variance *t*-test was used to select the significant altered genes (1754 genes) based on multivariate permutations test (1000 random permutations) at a nominal significance level of each univariate test of  $p \leq 0.001$ , maximum allowed number of false-positive genes of 10 at a confidence level of false discovery rate assessment of 90%. The significant genes were further filtered with the geometric mean intensities varied greater than or equal to fourfold over control (both directions) in at least one treatment. Hierarchical clustering analysis was conducted with the log<sub>2</sub> transformed ratio in the MEV (Saeed *et al.*, 2003) using average linkage and Euclidean dissimilarity (Eisen *et al.*, 1998). The columns represent treatments examined, whereas the genes and their expression values (fold change) are displayed in rows that are colored red if upregulated or green if downregulated. This analysis highlights common gene targets and similar changes in their expression between the metals and the classic proteasomal inhibitor. The array analysis determined that metals, in addition to MG132, induced significant impacts on specific gene clusters that include modulators of ubiquitin-proteasome functions (#), antioxidant and phase II detoxifying enzyme genes (\*), and cell cycle regulators (@).

(GOID 6281) were also significantly downregulated. Responses to stimulus especially to DNA damage stimulus (GOID 6974 and 9719) and immune response (GOID 6955) were also downregulated with Cd exposure. Cd significantly downregulated genes in oxidoreductase activity (GOID

16627 and 16637), metalloendopeptidase, and metallopeptidase activity (GOID 4222 and 8237). Downregulation in chromosome (GOID 5694, 786, and 775) and microbody genes (GOID 42579) such as peroxisome (GOID 5777) were significantly downregulated (Supplementary table 3B).

### *Common Shared Gene Expression Response to MG132, MeHg, and Cd*

We initially used nonsupervised two-dimensional hierarchical clustering analysis organized by gene and treatment to identify genes that share common patterns of expression across our metal treatments. By using the univariate *F*-test with random variance model, 2389 genes were observed to be significant ( $p < 0.001$ ). Furthermore, 1754 significant genes were selected based on a multivariate permutations test computed on 1000 random permutations at a false discovery rate assessment set at 90% and a maximum allowed number of false-positive genes set at 10. Hierarchical clustering was conducted for 497 genes whose average intensities varied greater than or equal to fourfold over the control in at least one treatment among the 1754 genes. As shown in Figure 4, each treatment forms a distinctive gene expression pattern. Clusters A and B are detailed views of the common alterations in gene expression either up (A) or down (B) observed in MEFs in response to exposures of MG132, MeHg, and Cd. As shown in cluster A, MG132, MeHg, and Cd induced significant impacts on specific gene clusters that include modulators of the UPS (@), such as *Uchl1* and *Ube2c*, and antioxidant and phase II detoxifying enzyme genes (#), such as *Gsta2*, *Gsta3*, *Gsta4*, as well as 1700012B18Rik, a gene previously known as oxidative stress-induced growth inhibitor 1 (*Osgin1*).

The majority of the commonly downregulated genes were cell cycle-related genes (\*). Metals and MG132 significantly downregulated a large number of cell cycle regulatory genes such as cyclins (*Ccnb1*, *Ccnb2*, and *Ccna2*), cyclin-dependent kinase inhibitor *Cdkn3*, and cell and division cycle (*Cdc20*, *Cdc25*, *Cdc25b*, *25c*, and *Cdca1*).

A canonical pathway-based analysis and comparison of pathways changed across treatments were conducted with IPA. The association between the significantly changed genes ( $p \leq 0.01$  and fold change  $\geq 1.5$ ) and the canonical pathway was determined based on a  $p$  value ( $p \leq 0.05$ ) calculated with Fisher's exact test. As shown in Figure 5, the middle bar graph represents the  $p$  value of the disturbed signaling pathway, the genes altered in each pathway were listed on the right side. Gene pathways such as the G<sub>2</sub>/M DNA cell cycle regulation pathway, oxidative-related responses pathways such as Nrf2-mediated oxidative stress response, GSH metabolism, and metabolism of xenobiotics by cytochrome P450, aryl hydrocarbon receptor signaling, protein ubiquitination pathway, as well as p38 MAPK signaling pathways were observed to be significantly changed across treatments (Fig. 5). As indicated in Figure 5, although we observed more genes changed with the Cd treatment, the log<sub>2</sub> value for the significance of  $p$  was lower than MG132 or MeHg.

### *Impacts of MG132, MeHg, and Cd on Nrf2-Mediated Oxidative Stress Response*

As shown in Figure 6A, MG132 treatment (0.5 μM for 24 h) in MEFs induced significant upregulation of genes in Nrf2-

mediated oxidative stress response, such as antioxidant and phase II detoxifying enzymes. Glutathione *S*-transferase (*Gsta2*, *Gsta3*, *Gsta4*, *Gstm1*, *Gstm2*, *Gstm3*, *Gstm5*, and *Mgst1*), glutamate-cysteine ligase (*Gclm*), glutathione reductase 1 (*Gsr*), glutathione synthetase (*Gss*), NAD(P)H dehydrogenase quinone 1 (*Noq1*), peroxiredoxin 1 (*Prdx1*), epoxide hydrolase (*Ephx1* and *Ephx2*), catalase (*Cat*), and superoxide dismutase 1 (*Sod1*) were significantly upregulated.

MeHg also induced significant alterations in transcription of genes involved in the antioxidant and phase II detoxification pathway (Fig. 6B). Significant upregulation of glutathione *S*-transferases (*Gsta2*, *Gsta3*, *Gsta4*, *Gsto1*, *Mgst1*), *Gclm*, *Gclc*, *Gsr*, *Gss*, *Noq1*, *Prdx1*, *Cat*, and superoxide dismutase 1 (*Sod1*) were observed with MeHg treatment (2.5 μM for 24 h). MeHg significantly upregulated a number of activating transcription factors, including *Atf2*, *Atf3*, *fos*, *fos*-like antigen 1s11 (*Fosl1*), as well as *Mafg* and *Mafk*. All these genes are involved in the activation of antioxidant-responsive elements (ARE). In contrast to MG132, MeHg significantly downregulated some forms of antioxidant and detoxification enzyme genes, such as glutathione *S*-transferase (*Gtm2*, *Gtm5*, *Gstk1*, and *Gstt1*), glutathione peroxidase (*Gpx1*, *Gpx3*, and *Gpx7*), isocitrate dehydrogenase 1 (NADP<sup>+</sup>) (*Idh1*), and NAD(P)H dehydrogenase quinone 2 (*Noq2*).

Similar to MeHg, Cd induced significant alterations in the transcription of genes involved in the antioxidant and phase II detoxification pathway (Fig. 6C). Significant upregulation of glutathione *S*-transferase (*Gsta2*, *Gsta3*, and *Gsta4*), *Gclm*, *Noq1*, *Prdx1*, and *Cat* were observed. Upregulation of a number of activating transcription factors such as *Atf1*, *Atf2*, *Atf3*, *Fosl1*, *Maf*, *Maff*, and *Mafk* were also observed. In contrast to MG132, Cd also reduced gene expression in some forms of antioxidant and detoxification enzyme genes, such as glutathione *S*-transferase (*Gstz1*, *Gstk1*, and *Gstt1*), glutathione peroxidase (*Gpx1* and *Gpx7*), and epoxide hydrolase (*Ephx1* and *Ephx2*). Moreover, Cd significantly downregulated kelch-like ECH-associated protein 1 (*Keap1*), a gene associated with Nrf2-mediated transcription.

### *Impacts of MG132, MeHg, and Cd on Cell Cycle Regulation Pathway*

MG132 induced significant upregulation of *Skp2* and cyclin E and downregulation of genes of cyclin A2, D3, cyclin-dependent kinase *Cdc2a*, cyclin-dependent kinase inhibitor p18 and p19, as well as serine/threonine protein kinase *Plk* in G<sub>1</sub>-S phase (Fig. 7A). In the G<sub>2</sub>/M phase (Fig. 7B, 1), MG132 induced significant upregulation of *Gadd45a* and *Mdm2*, in addition to the downregulation of cyclin B1/2, *Cdc20*, *Cdc25c*, *Cdc25b*, *Cdc2a*, and checkpoint kinase 1 (*Chk1*).

Although MeHg treatment appeared to affect genes in all stages of the cell cycle, the most significant effects were observed in G<sub>2</sub>/M phase transition as shown in Figure 7. In the G<sub>1</sub>-S phase, MeHg induced significant upregulation of *Smad3*, *Smad4*, *Abl1*, and *Gsk3b*, in addition to the downregulation of

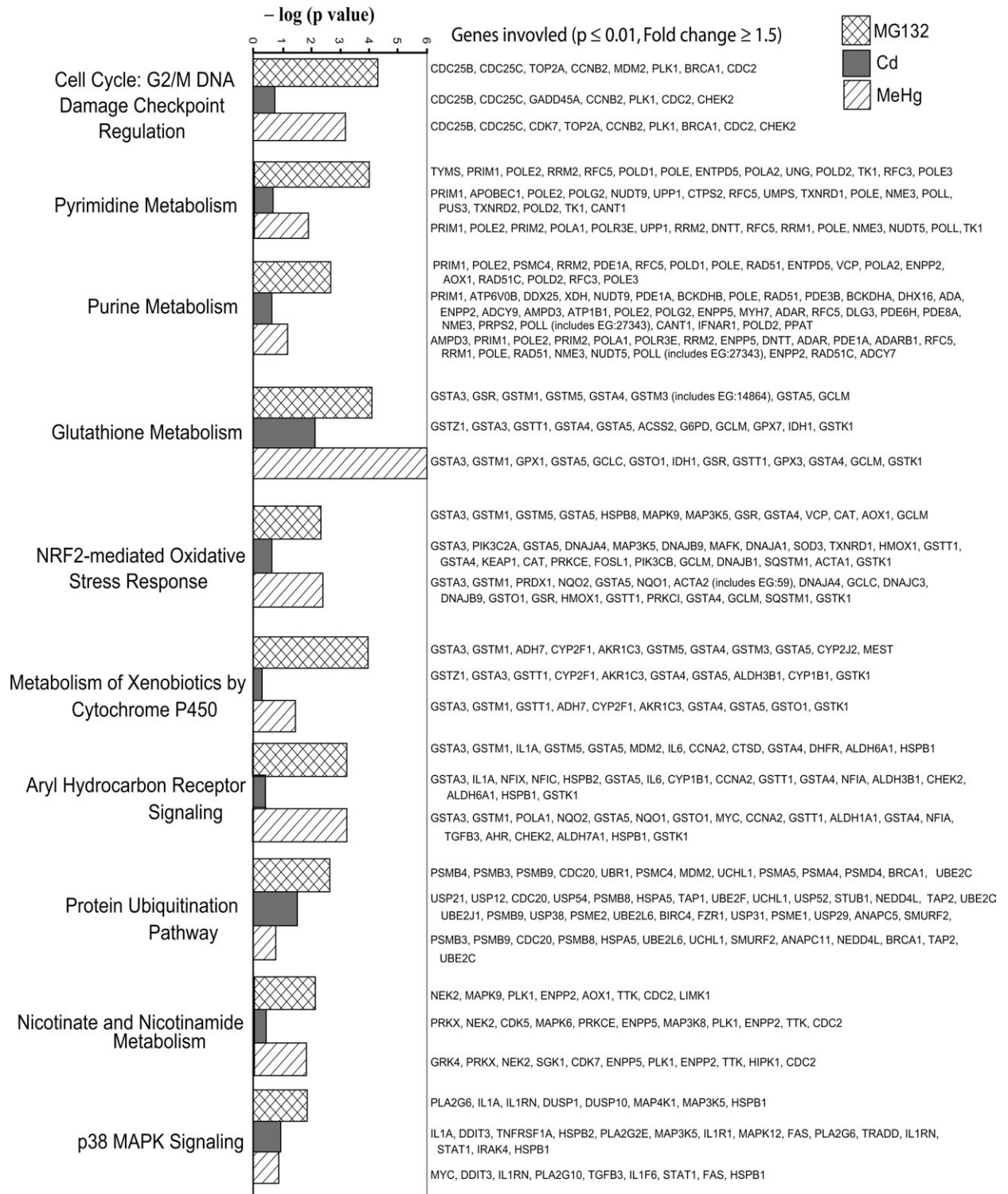


**FIG. 5.** Canonical pathway-based analyses of gene expression data in MEF cells exposed to MG132, methylmercury (MeHg), and cadmium (Cd). IPA (Ingenuity Systems, www.ingenuity.com) was used to identify the genes significantly associated with canonical pathways in the Ingenuity Pathways Knowledge Base. Genes from the each treatment that met the significance  $p$  value cutoff of 0.01 and fold change cutoff of 1.5 were associated with a canonical pathway in Ingenuity’s Knowledge Base were considered for the analysis. The significance of the association between the each treatment and the canonical pathway was measured in two steps. First, a ratio of the number of genes from each treatment that map to the pathway divided by the total number of genes that map to the canonical pathway is calculated. Then, Fisher’s exact test was used to calculate a  $p$  value determining the probability that the association between the genes in each treatment and the canonical pathway is explained by chance alone. MG132, MeHg, and Cd treatments induced alteration of Nrf2-mediated oxidative stress response, cell cycle and DNA damage checkpoint regulatory pathway, and ubiquitin-proteasomal regulatory pathways.

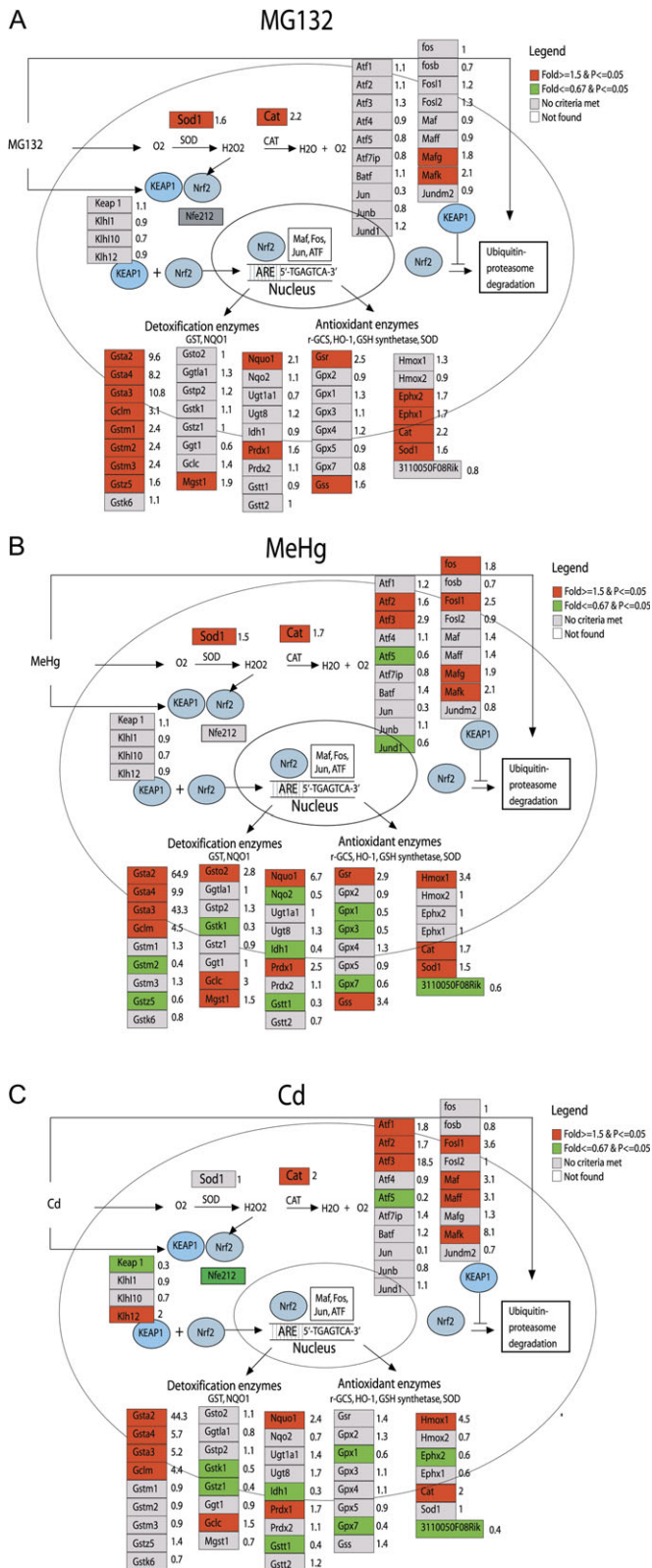


**FIG. 6.** Antioxidant and phase II detoxifying enzyme genes in response to MG132 (A), methylmercury (MeHg, B), and cadmium (Cd, C) in MEF cells. A knowledge-based pathway about antioxidant and phase II detoxifying enzyme regulation was built in GenMAPP program. Differential gene expression was

cyclin D3, E2, A2, cyclin-dependent kinase 1 (Cdc2a), cyclin-dependent kinase inhibitor p18 and p19, Plk1, and histone deacetylase 1 (Hdac1) (Fig. 7A, 2). In the G<sub>2</sub>/M phase, growth arrest and DNA damage-inducible genes (Gadd45a, Gadd45b, and Gadd45g) were upregulated, while cyclin B1, B2, Cdc20, Cdc25c, Cdc25b, Cdc2a, checkpoint kinase 1 (Chek1), Top2a, and wee1 were significantly downregulated (Fig. 7B, 2). The above changes in gene expression of the cell cycle regulators were similar to MG132.

The pattern of gene expression alerted by Cd in the cell cycle regulatory pathway was similar to that of MeHg. In the G<sub>1</sub>/S phase, Cd treatment induced the significant upregulation of cyclin A1 and Skp2, in addition to the downregulation of cyclin D3, E1, E2, A2, and Cdc2a. Additionally, cyclin-dependent kinase inhibitor p18 and p19 as well as Plk1 (Fig. 7A, 3) were downregulated. In the G<sub>2</sub>/M phase, Cd treatment significantly upregulated DNA damage-inducible genes, such as Gadd45a, Gadd45b, and Gad45g, Mdm2, Myt1, and Cdc25a. Conversely, cyclin B1, B2, Cdc20, Cdc25c, Cdc25b, Cdc2a, and Top2a were downregulated in the G<sub>2</sub>/M phase transition (Fig. 7B, 3).

*Impact of MG132, MeHg, and Cd on Ubiquitin-Proteasome Pathway*

As shown in Figure 8A, MG132—a nonspecific proteasome inhibitor—induced significant activation of proteasomal subunits of the 20S catalytic core and the 19S (PA700) regulatory complex. Additionally, we observed upregulation of the deubiquitination enzymes Uchl1, Ufd11, and Usp14. Ubiquitin E3 ligases were both upregulated (e.g., Nedd41, Fbxo6b, Skp1a, Skp2, Mdm2, ubr1, Rnf11) and downregulated (e.g., Fbx112, Siah1b, Siah2 and Lnx1). This suggests that MG132 treatment had a significant impact on a number of protein targets. MG132 also suppressed transcription in the ubiquitin activation enzyme Uble1a, conjugating enzymes (Ube2c, 2700084L22Rik), and proteasome subunit Psmb9.

In Figure 8B, MeHg induced significant activation of seven proteasome subunits of the 20S catalytic core and three subunits of the 19s (PA700) regulatory complex. In addition, MeHg induced upregulation of the deubiquitination enzymes (Uchl1, USP38, and Ufd11), the ubiquitin E3 enzymes (Nedd41, Skp1a, 4930431E10Rik, and Park2), and the ubiquitin-conjugating enzymes (Ube2e1, Arilh1, Arih2, Hip2, Ube2i, Ube2j1, 2510010F15Rik, and 6130401J04Rik). In contrast, MeHg suppressed transcription of the ubiquitin E3 ligase (Lnx1) and the ubiquitin-conjugating enzymes (Ube2c, Cblc,

based on treatment versus control expression change (1.5-fold and  $p \leq 0.05$ , *t*-test). Cd, MeHg, and MG132 treatment in MEF cell induced significant upregulation of glutathione S-transferase (Gsta2, Gsta3, and Gsta4), glutamate-cysteine ligase (Gclm), NAD(P)H dehydrogenase quinone 1 (Noq1), peroxiredoxin 1 (Prdx1), and catalase (Cat). In contrast to MG132, Cd uniquely significantly upregulated activating transcription factor (Atf1, Atf2, and Atf3), fos-like antigen 1s11 (Fosl1), Maf, Maff, and Maik. All these genes are involved in activation of ARE.

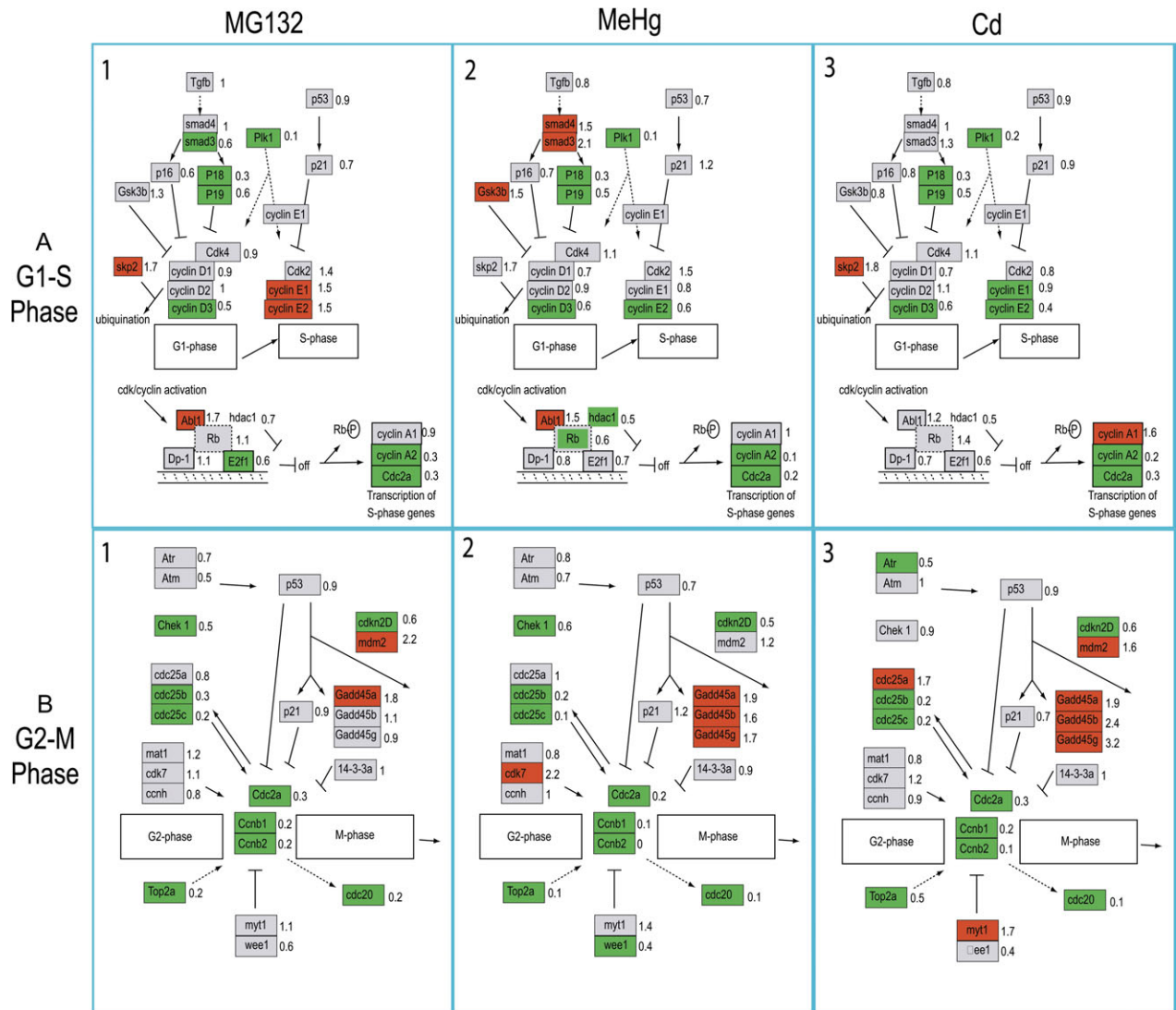


**FIG. 7.** Changes in cell cycle regulation in response to MG132 (A), methylmercury (MeHg, B), and cadmium (Cd, C) in MEF cells. Cell cycle regulation pathway was modified from KEGG in GenMAPP program. Differential gene expression was based on treatment versus control expression change (1.5-fold and  $p \leq 0.05$ , *t*-test). Red indicates a higher level of expression in the treatment. Green indicates decreased level of expression in the treatments. Gray indicates that the selection criteria were not met, but the gene is represented on the array. White boxes indicate that the gene was not present on the chip. Both Cd and MG132 treatment in MEF cell induced significant upregulation of Mdm2, Skp2, and Gadd45 and downregulation of genes mainly involving in  $G_2/M$  phase transition, such as cyclin B1/B2, cyclin A2, Cdk1, Cdc20, Cdc25c, Cdc25b, Chk2, Mad211, and Bub1.

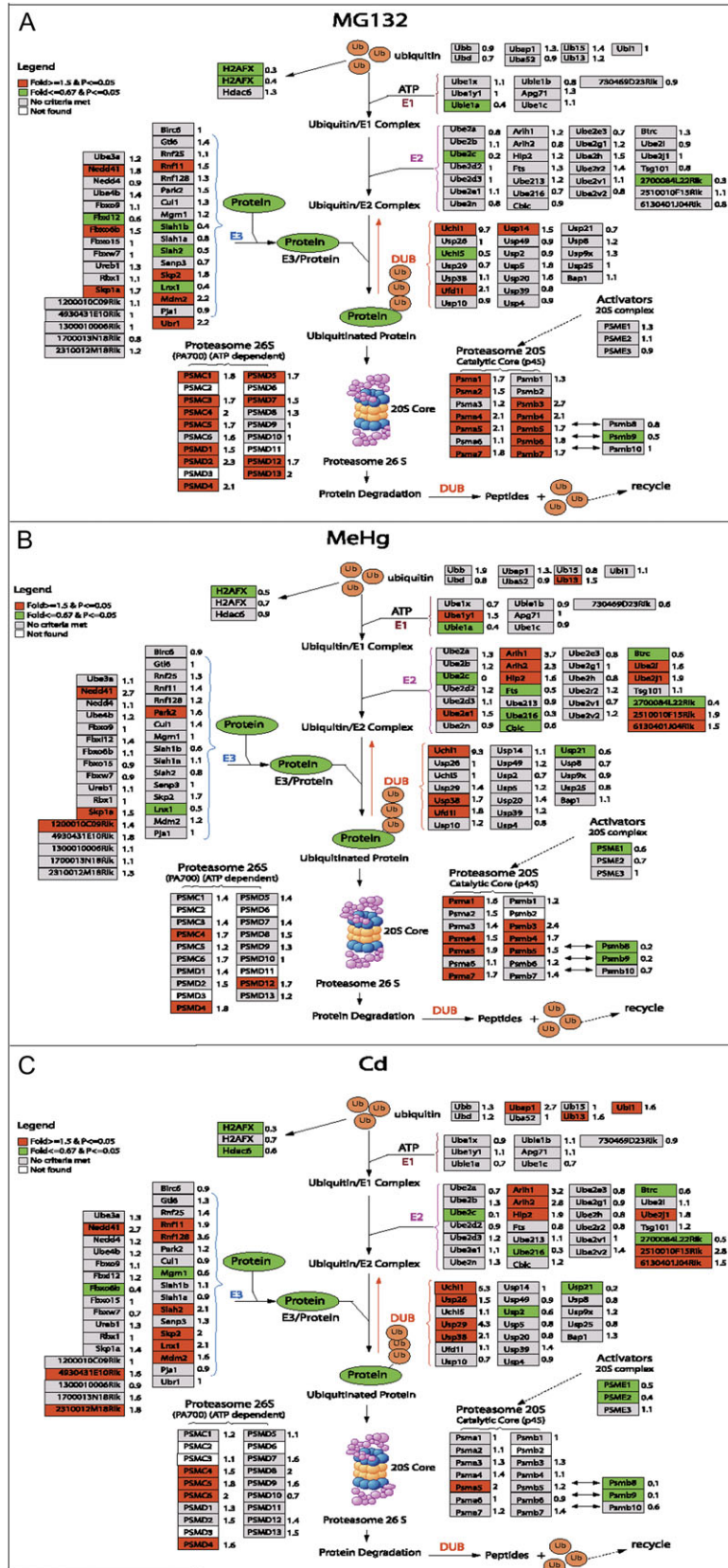
Ube216, Fts, Btrc, and 2700084L22Rik). Furthermore, MeHg suppressed transcription of the ubiquitin activation enzyme (Uble1a) proteasome activator of 20S complex, Psme1, and subunits Psmb8 and Psmb9.

In Figure 8C, as with MG132 and MeHg, Cd treatment induced significant upregulation of four subunits of the 19S (PA700) proteasome regulatory complex. Moreover, Cd significantly downregulated the proteasome subunits (Psm8 and Psm9) and the activators of the 20s complex (Psme1 and Psme2). Cd induced an increase in the transcription of deubiquitination enzymes Uchl1, Usp29, Usp26, and Usp38 and induced downregulation of the deubiquitination enzyme Usp2. The ubiquitin-conjugating enzymes Arlh1, Arih2, Hip2,

Ube2j1, 2510010F15Rik, and 6130401J04Rik were upregulated, while Ube2c, Ube216, Btrc, and 2700084L22Rik were downregulated. Cd also induced an increase in E3 enzymes Nedd4l, 4930431E10Rik, 2310012M18Rik, Rnf11, Rnf128, Siah2, Skp2, Mdm2, and Lnx1 but downregulated Fbxo6b and Mgrn1. Furthermore, Cd uniquely upregulated the ubiquitin-associated proteins Ubap1, ubl3, and Ubl1.

*PD Pathway Changes*

Kyoto Encyclopedia of Genes and Genomes (KEGG) pathways modified from GenMAPP software allow for the evaluation of collective gene expression changes associated with specific diseases. Figure 9 shows an example of this kind



of analysis for PD. Gene expression data from metal-treated MEFs were matched into the PD pathway modified from KEGG (2004) using GenMAPP software (Fig. 9). All three treatments upregulated the deubiquitination enzyme gene *Uchl1*, while the *Ube2c* and *270084L22Rik* genes were downregulated. Cd induced significant upregulation of the *Snca*, *Sncap*, and *MAPT* genes. The *Snca* gene, which produces the protein  $\alpha$ -synuclein, is a major component of Lewy bodies (LBs) and is the pathologic hallmark of PD (Kuhn *et al.*, 2003).

#### *Temporal Gene Expression Alterations by qRT-PCR in Response to MG132, MeHg, and Cd*

Table 2 shows the results from our qRT-PCR analyses across treatments of MG132, MeHg, and Cd. For our analysis, we used probes for *GST2a* from the antioxidant and phase II enzyme pathway; for *Uchl1* and *Ube2c* involved in the UPS pathway for *Ccnb1* and cell division *Cdc25c* from the cell cycle pathway; and lastly,  $\alpha$ -synuclein (*Snca*) from the PD pathway. Supplementary table 1 also shows the comparison of the fold changes of gene expression from the Codelink microarray and qRT-PCR resulting from 24 h of exposure to Cd, MeHg, or MG132. In general, for all of the six selected genes, consistent upregulation or downregulation with treatments were observed between the Codelink microarray and qRT-PCR expression values, with the exception of *Cdc25c* undergoing Cd treatment and *Snca* with MG132 treatment. Significant upregulation of *Gsta2*, *Uchl1* were both observed in Codelink array and qRT-PCR for Cd, MG132, and MeHg treatments. For the genes *Ube2c* and *Ccnb1*, significant downregulations in both Codelink array and qRT-PCR were observed. For the gene *Snca*, consistent upregulation in Cd treatment and downregulation in MeHg were observed, but for the MG132, no significant change was observed in Codelink array, while fivefold increase was observed in qRT-PCR. Significant decreases in gene expression of *Cdc25c* were observed in both Codelink array and qRT-PCR with MG132 and MeHg treatment. In Cd treatment, there was significant decrease in expression in Codelink array, but no change was observed in the qRT-PCR.

Next, we examined the temporal changes observed in the antioxidant and phase II enzymes (*Gsta2*, A), the PD-related genes (*Uchl1*, B, and *Snca*, C), and lastly, the cell cycle regulators (*Ccnb1*, D, and *Ube2c*, E) at 4, 8, and 24 h after treatment (Fig. 10). For the *Gsta2* gene, significant changes were observed for all treatments. Significant increases of *Gsta2*

were observed in the treatments with MeHg and MG132 at 8 and 24 h after treatments with more than 5- or 25-fold increases, respectively. In the treatment with Cd, *Gsta2* was observed to significantly increase over 40-fold 24 h after treatment. *Uchl1*, a deubiquitination enzyme that has been related to the PD pathogenesis, was found time dependently upregulated with peak at the 24-h time point for MeHg and MG132. Cd only slightly upregulated *Uchl1* at 24-h time point. MG132 time dependently upregulated *Snca* and significantly peaked at 24 h. Cd significantly upregulated *Snca* expression at 24 h after treatment with more than 14-fold upregulation. MeHg also significantly upregulated *Snca*, peaked at 4 h, and then returned to normal at 24 h. Genes *Ccnb1* and *Ube2c* were significantly downregulated in the Cd, MG132 treatment at 24 h, while in MeHg treatment, both *Ccnb1* and *Ube2c* significantly upregulated at 4 h, then downregulated at 24 h after treatment.

## DISCUSSION

### *Experimental Design*

In this study, we evaluated three treatment groups, including the two metals Cd and MeHg, and the proteasomal inhibitor MG132. Detailed cytotoxicity and cell cycle analysis studies were conducted to provide context for gene expression analysis. Our hypothesis was that the metals MeHg and Cd would significantly alter the UPS pathways and that these alterations might also have an effect on the neurodegenerative disease gene pathways. For the initial analyses, we chose minimally toxic concentrations of the agents for our gene expression comparison studies. MG132 (0.5 $\mu$ M) was included to provide a control to a known proteasomal inhibitor, allowing the assessment of UPS disruption characteristics for Cd and MeHg. We treated MEFs with environmentally relevant concentrations of MeHg (2.5 $\mu$ M) and Cd (5.0 $\mu$ M) for 24 h. The concentration of each metal is critical for the success of this study. If the metal concentration is too low, the effect on gene expression may be undetectable. Conversely, if the metal concentration is too high, the secondary effects could mask the primary response. The concentrations were selected based on our observations of morphology, while the NR uptake assay was based on cell viability. The concentrations of 0.5 $\mu$ M for MG132, 2.5 $\mu$ M for MeHg, and 5 $\mu$ M for Cd are the initial concentrations where we observed a significant decrease in the

← **FIG. 8.** Alteration in Ubiquitin-Proteasome System (UPS) in response to MG132 (A), methylmercury (MeHg, B), and cadmium (Cd, C) in MEF cells. A knowledge-based UPS pathway was built in GenMAPP program. Differential gene expression was based on treatment versus control expression change (1.5-fold and  $p \leq 0.05$ , *t*-test). Red or green indicates a significant upregulated or downregulated level of expression after treatment. Gray indicates that the selection criteria were not met, but the gene is presented on the array. White boxes indicate that the gene was not present on the chip. The comparison of the UPS pathway mapping among metals (Cd and MeHg) and proteasome inhibitor MG132 revealed both common and unique targets on the UPS in the MEF. Cd, MeHg, and MG132 treatment in MEF cell induced significant upregulation of proteasome regulatory complex 19s (PA700) and deubiquitination gene *Uchl1* and significant downregulation of ubiquitin-conjugating enzyme *Ube2C*, *270084L22Rik*.

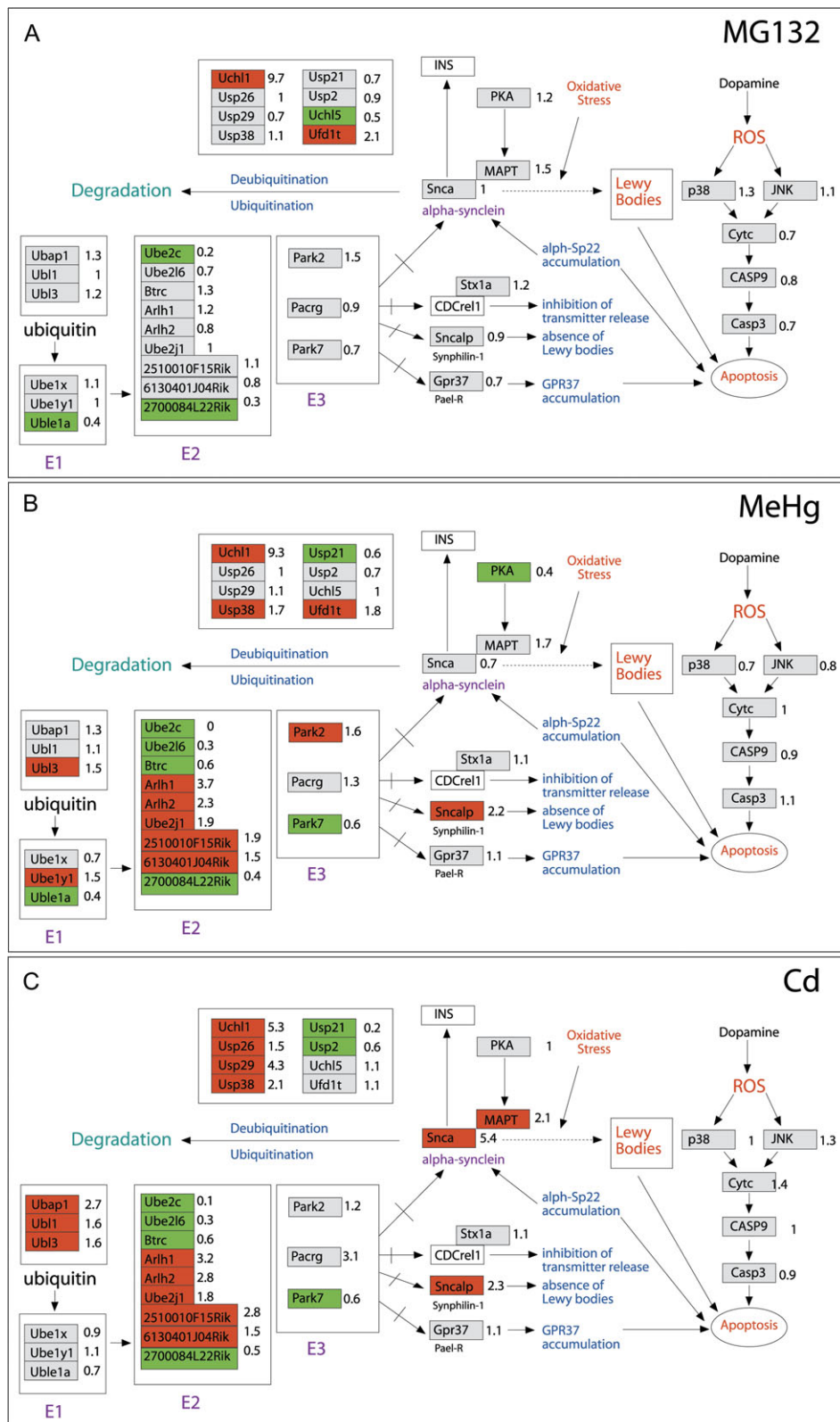


**FIG. 9.** Parkinson's disease (PD)-related gene pathway in response to MG132 (A), methylmercury (MeHg, B), and cadmium (Cd, C) in MEF cells. PD pathway was modified from KEGG in GenMAPP program. Differential gene expression was based on treatment versus control expression change (1.5-fold and  $p \leq 0.05$ ,  $t$ -test). All the treatments upregulate the deubiquitination enzyme gene Uch11 and downregulated Ube2c and 2700084L22Rik genes. Cd induced significant upregulation of Snca gene, which produce  $\alpha$ -synuclein protein, Sncalip, and MAPT genes.

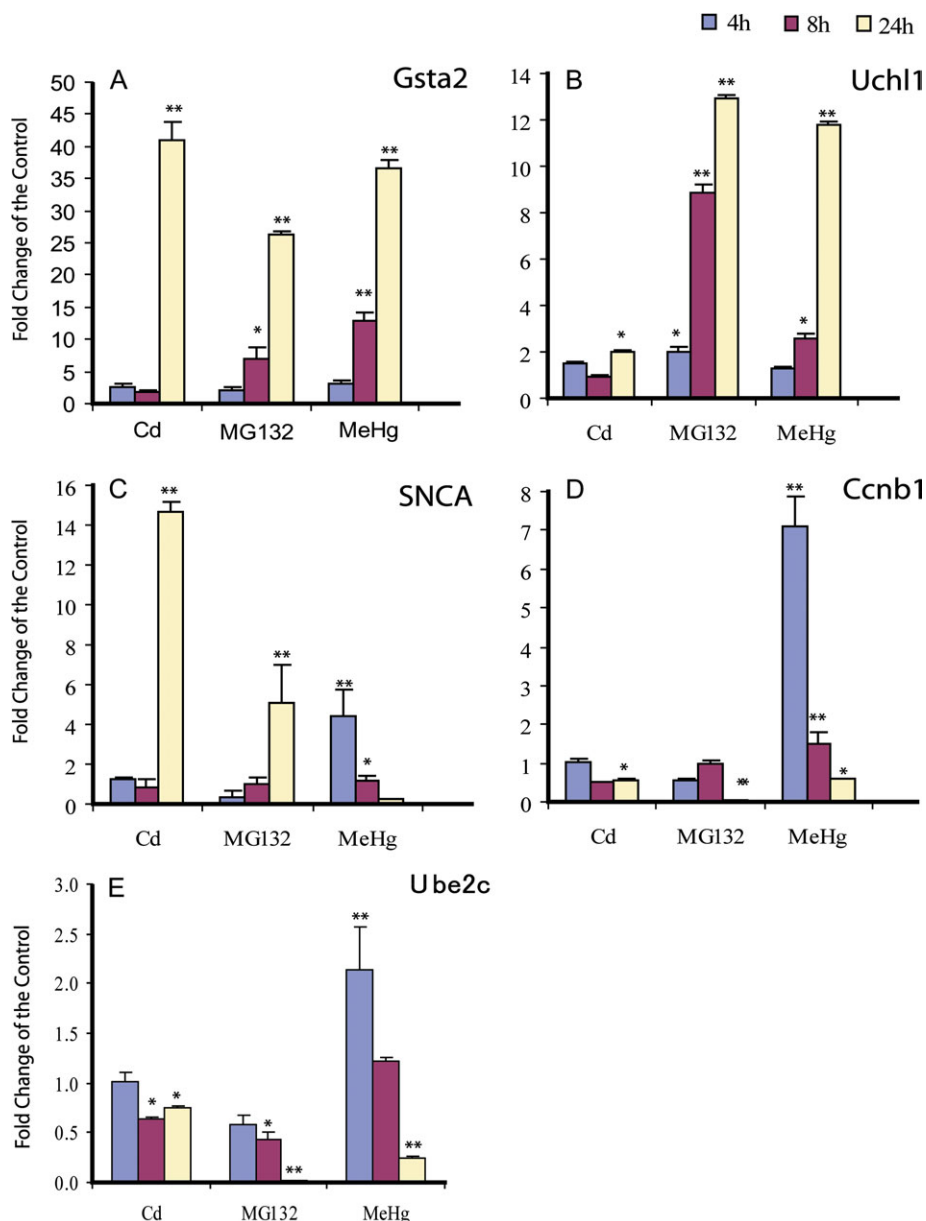


**FIG. 10.** Temporal gene expression alterations by qRT-PCR in response to cadmium (Cd), methylmercury (MeHg), and MG132 in MEF cells. Cultures of MEF cells were exposed to MeHg, MG132, and Cd for 4, 8, and 24 h, respectively. Following the exposure, cells were harvested and mRNA were extracted and qRT-PCR analysis of genes of Gsta2 (A), Uchl1 (B), Snca (C), Ccnb1 (D), and Ubec2 (E) were conducted as described in the “Materials and Methods” section. Statistical analysis was conducted using ANOVA, followed by Dunnett’s method to the control, with a significance level of  $p \leq 0.05$  (\*). Data are presented as mean  $\pm$  SE,  $n = 3$ .

cell viability of MEFs at 24 h. “Biological triplicates” were included in our experimental design. Three independent cell cultures and treatments were conducted simultaneously, three RNA samples were prepared, and three hybridizations were performed for each treatment.

Several proteasome-specific protease inhibitors have been used as model chemicals in order to investigate the role of the ubiquitin-proteasome protein degradation pathway and the biological processes dependent on this pathway (Koch *et al.*, 2009; Song *et al.*, 2009; Wu *et al.*, 2002; Zhang *et al.*, 2008).

In this study, we selected the 26S proteasome-specific protease inhibitor MG132 as a model chemical with which to explore genome-wide gene expression-associated alterations with proteasomal inhibition. Moreover, we were able to gather comprehensive pictures of pathways effected by the proteasome and compare the changes with those induced by metals. This allowed us to test our hypothesis that the disruption of the UPS pathway is an important mechanism involved in metal-induced toxicity. Inhibition of the proteasome results in the accumulation of unfolded polypeptides, which may trigger

the expression of HSPs, chaperones, and stress proteins of the endoplasmic reticulum. Transcriptional profiling with cDNA microarray analysis of human cancer cells exposed to the proteasome inhibitors lactacystin, lactacystin-beta-lactone, and MG132 showed the induction of heat-shock genes, gene encoding proteasome subunits, enzymes of amino acid, and polysaccharide metabolism as well as a number of unknown genes (Zimmermann *et al.*, 2000). Our current study characterized the global gene profile of a UPS model chemical MG132 and demonstrated that inhibition of the proteasome leads to alterations at the transcriptional level in genes associated with protein metabolism, oxidative stress, GSH activity, DNA damage, and cell cycle control. The changes of an important posttranslation modification UPS signaling pathway from the classic proteasome inhibitor MG132 confirmed that gene expression profiling is still a suitable tool in investigating the posttranslational modification. Further proteomic analysis is necessary to examine the specific proteins involving in the process of modification.

The functional interpretation of the pathway analysis of microarray-based gene expression is always challenging. In this study, we employed both GO analysis with GenMAPP and IPA approaches. Using these integrated tools, we identified significant gene expression changes across treatments within the UPS, antioxidant and phase II enzymes, and cell cycle regulation pathways. As shown in Figure 5, although we observed similar or more genes changed with the Cd treatment, the log 2 value of the significance  $p$  was lower than MG132 or MeHg. The calculation of the  $p$  value in the Fisher's exact test is corrected by the total number of genes changed. The number of genes changed after Cd treatment was the highest, followed by the MeHg and MG132 treatments.

#### *Nrf2-Mediated Oxidative Stress Response Pathway*

Our results demonstrated a significant alteration in Nrf2-mediated oxidative stress response after treatments with MG132, MeHg, and Cd (Figs. 5 and 6). The induction of antioxidant and phase II detoxifying enzymes acts as an important defense mechanism against environmental stressors. Oxidative stress has been shown not only to initiate the onset of disease, but it also exacerbates specific diseases, including cancer, Alzheimer's, atherosclerosis, diabetes, arthritis, and PD. Cells have well-developed antioxidant systems that help to protect them from reactive oxygen species. The cellular and molecular adaptive responses to oxidative stress involve increased expression of antioxidant enzymes, phase II detoxification enzymes, and stress-induced cytoprotective genes aimed at reversing the oxidant imbalance and achieving cellular homeostasis. The ability and efficacy of these adaptive responses to maintain redox homeostasis in large part dictates whether the cell or organ will survive the oxidant burden. Recent research has revealed that Nrf2 is essential for the coordinated transcriptional induction of various antioxidant and phase II detoxifying enzymes through the ARE (Long

*et al.*, 2001). ARE sequences have been characterized within the proximal regulatory sequences of genes encoding the antioxidant enzymes glutathione-S-transferase GST, NAD(P)H dehydrogenase quinone 1(NQO1), and heme oxygenase-1 (HO-1). ARE sequences also regulate a wide range of metabolic responses to oxidative stress caused by reaction oxidative stress. As a consequence of inadequate induction of these molecules, Nrf2-deficient mice are sensitive to high oxidative stress and drug-induced stress (Itoh *et al.*, 2004). Nrf2, which normally exists in an inactive state as a consequence of binding to Keap1, can be activated by redox-dependent stimuli. Alteration of the Nrf2-Keap1 interaction enables Nrf2 to translocate to the nucleus, bind to the ARE, and initiate the transcription of genes coding for detoxifying enzymes and cytoprotective proteins (Chan and Kan, 1999). Inhibition of proteasome activity by MG132 treatment (0.5 $\mu$ M for 24 h) induced significant upregulation of antioxidant and phase II detoxifying enzymes. MG132 and lactacystin have been found to selectively induce class p-GST isozyme (GST P1) (Usami *et al.*, 2005). In our tests, downregulation of proteasome by antisense or RNA interference resulted in a significant upregulation of GST P1, suggesting that a decline in the proteasome activity could, directly or indirectly, be linked to the induction of GST P1 (Usami *et al.*, 2005). Proteasome inhibition by lactacystin was reported to upregulate HSPs and molecular chaperones and respond to oxidative stress and cell cycle regulation (Yew *et al.*, 2005). Our microarray-based gene expression analysis suggests that inhibition of proteasome activity by MG132 reduces the capacity of the UPS-dependent clearance of unwanted proteins, leading to a broad range induction of antioxidant and phase II detoxifying enzymes.

Exposure to MeHg, *in vitro* and *in vivo*, has been reported to produce significant induction of genes involved in the antioxidant and phase II detoxification pathway (Ou *et al.*, 1999a; Sarafian, 1999; Thompson *et al.*, 2000; Woods and Ellis, 1995). In our tests, MeHg and Cd induced significant alterations in the transcription of genes involved in the antioxidant and phase II detoxification pathway. Cd treatment has been shown to alter Nrf2 degradation through the ubiquitin proteasome-dependent pathway (Stewart *et al.*, 2003). As demonstrated in Figure 6, although we observed that metals and MG132 treatment induced similar changes in Nrf2 pathways, striking differences in the expression of downstream genes exists. These differences might be dose related since the cell viability of Cd at 5 $\mu$ M and MeHg at 2.5 $\mu$ M is about 55%, while MG132 is about 80%. Further dose- or time-dependent examination will be valuable in defining Nrf2 pathways. In summary, comparisons of alterations in gene expression induced by MeHg, Cd, and MG132 in the antioxidant and phase II detoxification pathway infers the importance of this pathway in the development of adverse effects and the possible interaction between the UPS pathway.

### Cell Cycle Regulatory Pathway

The changes observed at the transcriptional level of cell cycle regulatory molecules induced by MeHg and Cd exhibit a strong similarity to the UPS disruptor MG132. Significant alterations of genes involved in cell cycle regulation were observed after treatments with MG132, MeHg, and Cd. The mammalian mitotic cell cycle involves a sequence of transitions and can be divided into four discrete phases: G<sub>1</sub>, S phase, G<sub>2</sub>, and M phase. The G<sub>1</sub> and G<sub>2</sub> phases serve as checkpoints for the cell to make sure that it is ready to proceed in the cell cycle. S phase involves the replication of chromosomes. The cell cycle is governed by sequential activation and inactivation of a family of cyclin-dependent kinases (cdks) (Sherr and Roberts, 1999). Cdk activation requires cyclin association. Cyclin levels typically oscillate throughout the cell cycle. Progression through G<sub>1</sub> into S phase is regulated by D-type cyclins associated with Cdk4 or Cdk6 and E-type cyclin E-Cdk2. Subsequently, as cells enter S phase, cyclin A-Cdk2 is activated. The cyclin B/Cdk2 complex controls the entry of mitosis (Tyers, 2004; Tyson *et al.*, 2002). The INK4 and the Cip/Kip inhibitors are two main families of cyclin-dependent kinase inhibitors (Ckis). The Cip/Kip family of inhibitors is composed of p21<sup>Cip1</sup>, p27<sup>Kip1</sup>, and p57<sup>Kip2</sup> and exhibit a broad range of inhibitory activity toward most Cdk-cyclin complexes (Morgan, 1995). In vertebrates, many regulators, including p27<sup>Kip1</sup>, p21<sup>Cip1</sup>, E2F, Cdc6, and cyclin E, B, A, and D1, are known to be targeted for UPS-dependent proteolysis. The inhibition of proteasome activity by MG132 resulted in a significant impact on cell cycle regulatory genes both in the G<sub>1</sub>-S and in the G<sub>2</sub>/M phases, suggesting the critical role of UPS in normal cell cycle progression. We observed a similar change in the gene expression of the cell cycle regulators in MeHg treatment. MeHg has been shown to inhibit cell cycle progression, causing an accumulation or arrest of cells in the G<sub>2</sub>/M transition (Maekawa *et al.*, 1999). Observations of change in the genes involved in growth arrest and DNA damage are consistent with our previous study, showing that mitosis (the G<sub>2</sub> accumulation) and synthesis of some macromolecules in G<sub>1</sub> are susceptible to MeHg exposure (Faustman *et al.*, 2002; Gribble *et al.*, 2005; Mendoza *et al.*, 2002; Ou *et al.*, 1997, 1999b; Ponce *et al.*, 1994; Vogel *et al.*, 1986). Our previous work with MeHg in neuronal cells isolated from rodent embryos detected a twofold increase in GADD153 gene expression by 2.0 μM MeHg after 24 h in primary cell cultures and a fivefold to eightfold increase in GADD45 expression postexposure (Ou *et al.*, 1997). Our recent work further demonstrated that MeHg-induced cell cycle arrest occurs via both p53-dependent and -independent pathways. Moreover, cell death resulting from MeHg exposure is highly dependent on p53 (Gribble *et al.*, 2005). Cd has also been reported to alter the cell cycle (Chung *et al.*, 2003; Vaughan *et al.*, 2001). This study suggests that the metal-induced neurotoxicity we have seen in our other studies is associated

with the perturbation of genes involved in the regulation of the cell cycle and the above changes can possibly be linked to the alteration of the UPS pathway.

### Interruptions of Ubiquitin-Proteasome Pathway

The UPS is a highly conserved cellular pathway that plays an important role in the selective degradation of cellular proteins that are essential for the regulation of a variety of vital cellular functions (Joazeiro and Hunter, 2000; Vabulas, 2007). Disruption of this system, therefore, can have significant downstream effects on critical cellular functions, impacting susceptibility and development of disease. Comparisons of the gene expression between the metals and proteasome inhibitor MG132 by microarray and qRT-PCR revealed the common targets in the UPS of the mouse embryonic cells. MeHg and Cd treatment in MEF cells induced significant alteration of UPS pathway genes, including the significant decrease of the ubiquitin-conjugating enzyme Ube2c and Ube2e and the proteasome subunit Psmb9, in addition to the upregulation of DUB enzyme Uchl1, Usp29, and Usp12. Results from this array data strongly support our hypothesis that the disruption of the UPS function is involved in metal-induced adverse effects and demonstrates potential gene targets in this pathway.

Recent studies highlight the critical role of the UPS in modulating metal-induced toxicity (Di and Tamas, 2007; Figueiredo-Pereira *et al.*, 1998; Kirkpatrick *et al.*, 2003; Stanhill *et al.*, 2006; Stewart *et al.*, 2003). By screening a yeast genomic DNA library, the overexpression of the ubiquitin-protein ligase CDC34 (E3) increased the cellular-ubiquitinated protein levels and exhibited significant resistance to MeHg toxicity both in yeast and in human cells (Furuchi *et al.*, 2002; Hwang *et al.*, 2002). The ubiquitin-conjugating activity of CDC34 is essential for the CDC34-mediated resistance to MeHg. This report suggests that MeHg induces the cellular accumulation of certain proteins that cause cell damage and that CDC34 is degraded after its ubiquitination in the proteasome (Furuchi *et al.*, 2002; Hwang *et al.*, 2002, 2005; Naganuma *et al.*, 2002).

Mouse neuronal HT4 cells—treated with Cd, zinc, and H<sub>2</sub>O<sub>2</sub>—have been reported to induce accumulation of ubiquitination and reduce GSH levels and/or increase protein-mixed disulfides, leading to a decrease in cell viability even after an overnight recovery period in the absence of treatment (Figueiredo-Pereira and Cohen, 1999). This report also shows the critical role of the UPS in the removal of proteins that are oxidatively modified and suggests that accumulation of ubiquitinated proteins in the cell contributes to an overall decrease in cell viability. Similarly, other heavy metals such as cobalt have been reported to induce the inhibition of proteasomal activity, leading to the accumulation of high molecular weight poly-ubiquitinated conjugates and apoptosis (Araya *et al.*, 2002). Previously reported studies have found a similar attenuation, suggesting the response to be a result of decreased enzyme activity associated with deubiquitination (Figueiredo-Pereira and Cohen, 1999; Figueiredo-Pereira *et al.*, 1998). Additional studies have

demonstrated that defects in the UPS-sensitized cells to Cd-mediated impacts (Tsirigotis *et al.*, 2001) and mutants in specific ubiquitin-conjugating enzymes are hypersensitive to Cd (Jungmann *et al.*, 1993; Wagenknecht *et al.*, 1999).

During the pathway mapping analysis of the gene expression induced by MG132, Cd, and MeHg, significant alterations were found in the PD pathway. PD is thought to result from a complex interaction between multiple predisposing genes and environmental influences; however, these interactions are still poorly understood. Causative genes have been identified in different families (Polymeropoulos, 2000). The etiology of PD is likely to be multifactorial, a complex interplay between genetic factors and environmental factors (Dawson and Dawson, 2003; McNaught *et al.*, 2003). Oxidative stress and the impairment of UPS-dependent protein degradation processing have both been identified as the main pathophysiological factors involved in degenerative processes associated with PD (Moore *et al.*, 2003; Ohdate *et al.*, 2003). Our results show that all three treatments upregulated the deubiquitination enzyme gene *Uchl1* and downregulated *Ube2c* and *270084L22Rik* genes. Cd induced significant upregulation of *Sncg* gene as well as the *Sncap* and *MAPT* genes. The *Sncg* gene, which produces the protein  $\alpha$ -synuclein, is a major component of LBs and the pathologic hallmarks of PD (Kuhn *et al.*, 2003). Upregulation of *Uchl1* mRNA,  $\alpha$ -synuclein, *Parkin*, and *HSP70* have been reported in mice 2 h after second injection of 15 mg/kg 1-methyl-4-phenyl-1,2,3,6-tetrahydropyridine (MPTP) (Kuhn *et al.*, 2003). *Uchl1* is a member of a gene family whose products hydrolyze small C-terminal adducts of ubiquitin to generate the ubiquitin monomer. It is highly conserved across species and is predominantly expressed within neurons and testicular tissue (Kwon *et al.*, 2005; Mochida *et al.*, 2004). The *Uchl1* enzyme was first defined in the context of familial and sporadic forms of the PD where it plays a pathological role in the formation of inclusions (Chung *et al.*, 2003; Maraganore *et al.*, 2004; Wintermeyer *et al.*, 2000). A significant inverse association of the *Uchl1* S18Y polymorphism with PD overall and in several strata has been observed, confirming its role as a susceptibility gene for PD (Facheris *et al.*, 2005; Maraganore *et al.*, 2004). The protein level of *Uchl1* is found to be downregulated in idiopathic PD as well as Alzheimer's disease brains (Choi *et al.*, 2004). In addition, Barrachina *et al.* (2006) found that reduced *Uchl1* expression was a contributory factor to the development of abnormal protein aggregation in dementia with Lewy bodies (DLB) and suggested *Uchl1* as a putative therapeutic target in the treatment of DLB (Barrachina *et al.*, 2006). Liu *et al.* (2002) found that within cultured cells *Uchl1* variants linked to higher susceptibility to PD caused the accumulation of  $\alpha$ -synuclein (Liu *et al.*, 2002). The above gene alterations, specifically those induced by Cd, are similar to those induced by the PD model chemical MPTP in mice.

Although the analysis of gene expression by microarray cannot completely reflect the changes of protein levels, such as

posttranslational modification, our gene expression profiling result from classical proteasome inhibitor MG132 reflects the changes of the UPS signaling pathway, an important posttranslational modification. Further comparative proteomic analysis across metals and MG132 might provide insight into the specific proteins involved in UPS modification. Although relatively less toxic doses were used in the current gene expression analysis, a wide dose range study—including environment relevant dose—is needed to further examine the association of metal exposure, disruption of UPS, and neurotoxicity. MEFs have been widely used to investigate the molecular mechanism of metal-induced cell cycle arrest, apoptosis, and the role of p53; however, cell type-specific alterations—such as neuronal cells after metal treatment—need to be further addressed (Gribble *et al.*, 2003, 2005; Sidhu *et al.*, 2003; Yu *et al.*, 2008b).

In summary, the comparison of alterations in gene expression between the metals, Cd and MeHg, and the proteasomal inhibitor MG132 revealed both common and unique targets in the UPS. Although the involvement of the UPS pathway might be different among various cell types, the results of our microarray analysis using MEFs strongly suggests that the disruption of UPS function is an important mechanism in metal-induced toxicity, and the upregulation of *Sncg* by metals further suggests that metal exposure might be involved in the development of PD.

#### SUPPLEMENTARY DATA

Supplementary data are available online at <http://toxsci.oxfordjournals.org/>.

#### FUNDING

National Institute of Environmental Health Sciences (NIEHS) for Toxicogenomic grant; the U.S. Environmental Protection Agency (USEPA)-NIEHS University of Washington (UW) Center for Child Environmental Health Risks Research (USEPA and NIEHS 1P01ES09601); the NIEHS R01-ES10613, UW NIEHS Center for Ecogenetics and Environmental Health (5 P30 ES07033), and the Institute for Evaluating Health Risks.

#### ACKNOWLEDGMENTS

The authors wish to express their gratitude to Sean Quigley and Hannah Viernes in the Functional Genomics Laboratory for their excellent assistance with the microarray and qRT-PCR analyses.

#### REFERENCES

Araya, J., Maruyama, M., Inoue, A., Fujita, T., Kawahara, J., Sassa, K., Hayashi, R., Kawagishi, Y., Yamashita, N., Sugiyama, E., *et al.* (2002).

- Inhibition of proteasome activity is involved in cobalt-induced apoptosis of human alveolar macrophages. *Am. J. Physiol. Lung Cell. Mol. Physiol.* **283**, L849–L858.
- Barrachina, M., Castano, E., Dalfo, E., Maes, T., Buesa, C., and Ferrer, I. (2006). Reduced ubiquitin C-terminal hydrolase-1 expression levels in dementia with Lewy bodies. *Neurobiol. Dis.* **22**, 265–273.
- Basun, H., Lind, B., Nordberg, M., Nordstrom, M., Bjorksten, K. S., and Winblad, B. (1994). Cadmium in blood in Alzheimer's disease and non-demented subjects: results from a population-based study. *Biometals* **7**, 130–134.
- Bergomi, M., Vinceti, M., Nacci, G., Pietrini, V., Bratter, P., Alber, D., Ferrari, A., Vescovi, L., Guidetti, D., Sola, P., et al. (2002). Environmental exposure to trace elements and risk of amyotrophic lateral sclerosis: a population-based case-control study. *Environ. Res.* **89**, 116–123.
- Bertin, G., and Averbeck, D. (2006). Cadmium: cellular effects, modifications of biomolecules, modulation of DNA repair and genotoxic consequences (a review). *Biochimie* **88**, 1549–1559.
- Beyersmann, D., and Hechtenberg, S. (1997). Cadmium, gene regulation, and cellular signalling in mammalian cells. *Toxicol. Appl. Pharmacol.* **144**, 247–261.
- Burbacher, T. M., Grant, K. S., Mayfield, D. B., Gilbert, S. G., and Rice, D. C. (2005). Prenatal methylmercury exposure affects spatial vision in adult monkeys. *Toxicol. Appl. Pharmacol.* **208**, 21–28.
- Burbacher, T. M., Rodier, P. M., and Weiss, B. (1990). Methylmercury developmental neurotoxicity: a comparison of effects in humans and animals. *Neurotoxicol. Teratol.* **12**, 191–202.
- Castoldi, A. F., Coccini, T., and Manzo, L. (2003). Neurotoxic and molecular effects of methylmercury in humans. *Rev. Environ. Health* **18**, 19–31.
- Chan, K., and Kan, Y. W. (1999). Nrf2 is essential for protection against acute pulmonary injury in mice. *Proc. Natl. Acad. Sci. U.S.A.* **96**, 12731–12736.
- Chang, C. C., and Huang, P. C. (1996). Semi-empirical simulation of Zn/Cd binding site preference in the metal binding domains of mammalian metallothionein. *Protein Eng.* **9**, 1165–1172.
- Choi, B. H., Lapham, L. W., Amin-Zaki, L., and Saleem, T. (1978). Abnormal neuronal migration, deranged cerebral cortical organization, and diffuse white matter astrocytosis of human fetal brain: a major effect of methylmercury poisoning in utero. *J. Neuropathol. Exp. Neurol.* **37**, 719–733.
- Choi, J., Levey, A. I., Weintraub, S. T., Rees, H. D., Gearing, M., Chin, L. S., and Li, L. (2004). Oxidative modifications and down-regulation of ubiquitin carboxyl-terminal hydrolase L1 associated with idiopathic Parkinson's and Alzheimer's diseases. *J. Biol. Chem.* **279**, 13256–13264.
- Chung, K. K., Dawson, V. L., and Dawson, T. M. (2003). New insights into Parkinson's disease. *J. Neurol.* **250**(Suppl. 3), III15–III24.
- Clarkson, T. W. (1987). Metal toxicity in the central nervous system. *Environ. Health Perspect.* **75**, 59–64.
- Dawson, T. M., and Dawson, V. L. (2003). Molecular pathways of neurodegeneration in Parkinson's disease. *Science* **302**, 819–822.
- De Vrij, F. M., Sluijs, J. A., Gregori, L., Fischer, D. F., Hermens, W. T., Goldgaber, D., Verhaagen, J., Van Leeuwen, F. W., and Hol, E. M. (2001). Mutant ubiquitin expressed in Alzheimer's disease causes neuronal death. *FASEB J.* **15**, 2680–2688.
- Di, Y., and Tamas, M. J. (2007). Regulation of the arsenic-responsive transcription factor Yap8p involves the ubiquitin-proteasome pathway. *J Cell Sci.* **120**, 256–264.
- Diaz, D., Krejsa, C. M., White, C. C., Keener, C. L., Farin, F. M., and Kavanagh, T. J. (2001). Tissue specific changes in the expression of glutamate-cysteine ligase mRNAs in mice exposed to methylmercury. *Toxicol. Lett.* **122**, 119–129.
- Doniger, S. W., Salomonis, N., Dahlquist, K. D., Vranizan, K., Lawlor, S. C., and Conklin, B. R. (2003). MAPPFinder: using gene ontology and GenMAPP to create a global gene-expression profile from microarray data. *Genome Biol.* **4**, R7.
- Eisen, M. B., Spellman, P. T., Brown, P. O., and Botstein, D. (1998). Cluster analysis and display of genome-wide expression patterns. *Proc. Natl. Acad. Sci. U.S.A.* **95**, 14863–14868.
- Elinder, C. G., Edling, C., Lindberg, E., Kagedal, B., and Vesterberg, O. (1985). Assessment of renal function in workers previously exposed to cadmium. *Br. J. Ind. Med.* **42**, 754–760.
- Ercal, N., Gurer-Orhan, H., and Aykin-Burns, N. (2001). Toxic metals and oxidative stress part I: mechanisms involved in metal-induced oxidative damage. *Curr. Top. Med. Chem.* **1**, 529–539.
- Facheris, M., Strain, K. J., Lesnick, T. G., de Andrade, M., Bower, J. H., Ahlskog, J. E., Cunningham, J. M., Lincoln, S., Farrer, M. J., Rocca, W. A., et al. (2005). UCHL1 is associated with Parkinson's disease: a case-unaffected sibling and case-unrelated control study. *Neurosci. Lett.* **381**, 131–134.
- Faustman, E. M., Ponce, R. A., Ou, Y. C., Mendoza, M. A., Lewandowski, T., and Kavanagh, T. (2002). Investigations of methylmercury-induced alterations in neurogenesis. *Environ. Health Perspect.* **110**(Suppl. 5), 859–864.
- Figueiredo-Pereira, M. E., and Cohen, G. (1999). The ubiquitin/proteasome pathway: friend or foe in zinc-, cadmium-, and H<sub>2</sub>O<sub>2</sub>-induced neuronal oxidative stress. *Mol. Biol. Rep.* **26**, 65–69.
- Figueiredo-Pereira, M. E., Li, Z., Jansen, M., and Rockwell, P. (2002). N-acetylcysteine and celecoxib lessen cadmium cytotoxicity which is associated with cyclooxygenase-2 up-regulation in mouse neuronal cells. *J. Biol. Chem.* **277**, 25283–25289.
- Figueiredo-Pereira, M. E., Yakushin, S., and Cohen, G. (1998). Disruption of the intracellular sulfhydryl homeostasis by cadmium-induced oxidative stress leads to protein thiolation and ubiquitination in neuronal cells. *J. Biol. Chem.* **273**, 12703–12709.
- Fonnum, F., and Lock, E. A. (2004). The contributions of excitotoxicity, glutathione depletion and DNA repair in chemically induced injury to neurones: exemplified with toxic effects on cerebellar granule cells. *J. Neurochem.* **88**, 513–531.
- Forloni, G., Terreni, L., Bertani, I., Fogliarino, S., Invernizzi, R., Assini, A., Ribizzi, G., Negro, A., Calabrese, E., Volonte, M. A., et al. (2002). Protein misfolding in Alzheimer's and Parkinson's disease: genetics and molecular mechanisms. *Neurobiol. Aging* **23**, 957.
- Furuchi, T., Hwang, G. W., and Naganuma, A. (2002). Overexpression of the ubiquitin-conjugating enzyme Cdc34 confers resistance to methylmercury in *Saccharomyces cerevisiae*. *Mol. Pharmacol.* **61**, 738–741.
- Goering, P. L., Kuester, R. K., Neale, A. R., Chapekar, M. S., Zaremba, T. G., Gordon, E. A., and Hitchins, V. M. (2000). Effects of particulate and soluble cadmium species on biochemical and functional parameters in cultured murine macrophages. *In Vitro. Mol. Toxicol.* **13**, 125–136.
- Gribble, E. J., Hong, S. W., and Faustman, E. M. (2005). The magnitude of methylmercury-induced cytotoxicity and cell cycle arrest is p53-dependent. *Birth Defects Res. A Clin. Mol. Teratol.* **73**, 29–38.
- Gribble, E. J., Mendoza, A., Hong, S., Sidhu, J., and Faustman, E. M. (2003). Evaluation of cell cycle kinetics in p53 mouse embryonal fibroblasts: effects of methyl mercury. *Toxicol. Sci.* **72**, 67.
- Hershko, A., and Ciechanover, A. (1998). The ubiquitin system. *Annu. Rev. Biochem.* **67**, 425–479.
- Hwang, G. W., Furuchi, T., and Naganuma, A. (2002). A ubiquitin-proteasome system is responsible for the protection of yeast and human cells against methylmercury. *FASEB J.* **16**, 709–711.
- Hwang, G. W., Sasaki, D., and Naganuma, A. (2005). Overexpression of Rad23 confers resistance to methylmercury in *saccharomyces cerevisiae* via inhibition of the degradation of ubiquitinated proteins. *Mol. Pharmacol.* **68**, 1074–1078.

- International Agency for Research on Cancer. (2009). Cadmium and cadmium compounds. Available at <http://monographs.iarc.fr/ENG/Monographs/vol58/volume58.pdf>. Accessed January 20, 2010.
- Iseki, E., Odawara, T., Li, F., Kosaka, K., Nishimura, T., Akiyama, H., and Ikeda, K. (1996). Age-related ubiquitin-positive granular structures in nondemented subjects and neurodegenerative disorders. *J. Neurol. Sci.* **142**, 25–29.
- Itoh, K., Tong, K. I., and Yamamoto, M. (2004). Molecular mechanism activating Nrf2-Keap1 pathway in regulation of adaptive response to electrophiles. *Free Radic. Biol. Med.* **36**, 1208–1213.
- Joazeiro, C. A., and Hunter, T. (2000). Biochemistry. Ubiquitination—more than two to tango. *Science* **289**, 2061–2062.
- Jungmann, J., Reins, H. A., Schobert, C., and Jentsch, S. (1993). Resistance to cadmium mediated by ubiquitin-dependent proteolysis. *Nature* **361**, 369–371.
- Kirkpatrick, D., Dale, K., Catania, J., and Gandolfi, A. (2003). Low-level arsenite causes accumulation of ubiquitinated proteins in rabbit renal cortical slices and HERK293 cells. *Toxicol. and Applied Pharmacol.* **186**, 101–109.
- Koch, A., Lehmann-Horn, K., Dachsel, J. C., Gasser, T., Kahle, P. J., and Lucking, C. B. (2009). Proteasomal inhibition reduces parkin mRNA in PC12 and SH-SY5Y cells. *Parkinsonism Relat. Disord.* **15**, 220–225.
- Kuhn, K., Wellen, J., Link, N., Maskri, L., Lubbert, H., and Stichel, C. C. (2003). The mouse MPTP model: gene expression changes in dopaminergic neurons. *Eur. J. Neurosci.* **17**, 1–12.
- Kwon, J., Mochida, K., Wang, Y. L., Sekiguchi, S., Sankai, T., Aoki, S., Ogura, A., Yoshikawa, Y., and Wada, K. (2005). Ubiquitin C-terminal hydrolase L-1 is essential for the early apoptotic wave of germinal cells and for sperm quality control during spermatogenesis. *Biol. Reprod.* **73**, 29–35.
- Kyoto Encyclopedia of Genes and Genomes (KEGG). (2004). Available at <http://www.genome.jp/kegg/pathway/hsa/hsa05020.html>. Accessed January 20, 2010.
- Lam, Y. A., Pickart, C. M., Alban, A., Landon, M., Jamieson, C., Ramage, R., Mayer, R. J., and Layfield, R. (2000). Inhibition of the ubiquitin-proteasome system in Alzheimer's disease. *Proc. Natl. Acad. Sci. U.S.A.* **97**, 9902–9906.
- Lin, Y. S., Dowling, A. L., Quigley, S. D., Farin, F. M., Zhang, J., Lamba, J., Schuetz, E. G., and Thummel, K. E. (2002). Co-regulation of CYP3A4 and CYP3A5 and contribution to hepatic and intestinal midazolam metabolism. *Mol. Pharmacol.* **62**, 162–172.
- Liu, Y., Fallon, L., Lashuel, H. A., Liu, Z., and Lansbury, P. T., Jr. (2002). The UCH-L1 gene encodes two opposing enzymatic activities that affect alpha-synuclein degradation and Parkinson's disease susceptibility. *Cell* **111**, 209–218.
- Long, A. D., Mangalam, H. J., Chan, B. Y., Toller, L., Hatfield, G. W., and Baldi, P. (2001). Improved statistical inference from DNA microarray data using analysis of variance and a Bayesian statistical framework. Analysis of global gene expression in *Escherichia coli* K12. *J. Biol. Chem.* **276**, 19937–19944.
- Lowe, S. W., Jacks, T., Housman, D. E., and Rulley, H. E. (1994). Abrogation of oncogene-associated apoptosis allows transformation of p53-deficient cells. *Proc. Natl. Acad. Sci. U.S.A.* **91**, 2026–2030.
- Maekawa, T., Bernier, F., Sato, M., Nomura, S., Singh, M., Inoue, Y., Tokunaga, T., Imai, H., Yokoyama, M., Reimold, A., et al. (1999). Mouse ATF-2 null mutants display features of a severe type of meconium aspiration syndrome. *J. Biol. Chem.* **274**, 17813–17819.
- Maraganore, D. M., Lesnick, T. G., Elbaz, A., Chartier-Harlin, M. C., Gasser, T., Kruger, R., Hattori, N., Mellick, G. D., Quattrone, A., Satoh, J., et al. (2004). UCHL1 is a Parkinson's disease susceptibility gene. *Ann. Neurol.* **55**, 512–521.
- McNaught, K. S., Belizaire, R., Isacson, O., Jenner, P., and Olanow, C. W. (2003). Altered proteasomal function in sporadic Parkinson's disease. *Exp. Neurol.* **179**, 38–46.
- Mendoza, M. A., Ponce, R. A., Ou, Y. C., and Faustman, E. M. (2002). p21(WAF1/CIP1) inhibits cell cycle progression but not G2/M-phase transition following methylmercury exposure. *Toxicol. Appl. Pharmacol.* **178**, 117–125.
- Mochida, K., Ohkubo, N., Matsubara, T., Ito, K., Kakuno, A., and Fujii, K. (2004). Effects of endocrine-disrupting chemicals on expression of ubiquitin C-terminal hydrolase mRNA in testis and brain of the Japanese common goby. *Aquat. Toxicol.* **70**, 123–136.
- Moore, D. J., Dawson, V. L., and Dawson, T. M. (2003). Role for the ubiquitin-proteasome system in Parkinson's disease and other neurodegenerative brain amyloidoses. *Neuromolecular Med.* **4**, 95–108.
- Morgan, D. O. (1995). Principles of CDK regulation. *Nature* **374**, 131–134.
- Naganuma, A., Furuchi, T., Miura, N., Hwang, G. W., and Kuge, S. (2002). Investigation of intracellular factors involved in methylmercury toxicity. *Tohoku J. Exp. Med.* **196**, 65–70.
- The National Research Council (NRC). (2000). *Toxicological Effects of Methylmercury*. National Academy Press, Washington, DC.
- Ohdate, H., Lim, C. R., Kokubo, T., Matsubara, K., Kimata, Y., and Kohno, K. (2003). Impairment of the DNA binding activity of the TATA-binding protein renders the transcriptional function of Rvb2p/Tih2p, the yeast RuvB-like protein, essential for cell growth. *J. Biol. Chem.* **278**, 14647–14656.
- Okuda, B., Iwamoto, Y., Tachibana, H., and Sugita, M. (1997). Parkinsonism after acute cadmium poisoning. *Clin. Neurol. Neurosurg.* **99**, 263–265.
- Ou, Y. C., Thompson, S. A., Kirchner, S. C., Kavanagh, T. J., and Faustman, E. M. (1997). Induction of growth arrest and DNA damage-inducible genes Gadd45 and Gadd153 in primary rodent embryonic cells following exposure to methylmercury. *Toxicol. Appl. Pharmacol.* **147**, 31–38.
- Ou, Y. C., Thompson, S. A., Ponce, R. A., Schroeder, J., Kavanagh, T. J., and Faustman, E. M. (1999b). Induction of the cell cycle regulatory gene p21 (Waf1, Cip1) following methylmercury exposure *in vitro* and *in vivo*. *Toxicol. Appl. Pharmacol.* **157**, 203–212.
- Ou, Y. C., White, C. C., Krejsa, C. M., Ponce, R. A., Kavanagh, T. J., and Faustman, E. M. (1999a). The role of intracellular glutathione in methylmercury-induced toxicity in embryonic neuronal cells. *Neurotoxicology* **20**, 793–804.
- Philbert, M. A., Billingsley, M. L., and Reuhl, K. R. (2000). Mechanisms of injury in the central nervous system. *Toxicol. Pathol.* **28**, 43–53.
- Polymeropoulos, M. H. (2000). Genetics of Parkinson's disease. *Ann. N. Y. Acad. Sci.* **920**, 28–32.
- Ponce, R. A., Kavanagh, T. J., Mottet, N. K., Whittaker, S. G., and Faustman, E. M. (1994). Effects of methyl mercury on the cell cycle of primary rat CNS cells *in vitro*. *Toxicol. Appl. Pharmacol.* **127**, 83–90.
- Ramana, C. V., Kumar, A., and Enelow, R. (2005). Stat1-independent induction of SOCS-3 by interferon-gamma is mediated by sustained activation of Stat3 in mouse embryonic fibroblasts. *Biochem. Biophys. Res. Commun.* **327**, 727–733.
- Robinson, J. F., Yu, X., Hong, S., Griffith, W. C., Beyer, R., Kim, E., and Faustman, E. M. (2009). Cadmium-induced differential toxicogenomic response in resistant and sensitive mouse strains undergoing neurulation. *Toxicol. Sci.* **107**, 206–219.
- Saeed, A. I., Sharov, V., White, J., Li, J., Liang, W., Bhagabati, N., Braisted, J., Klapa, M., Currier, T., Thiagarajan, M., et al. (2003). TM4: a free, open-source system for microarray data management and analysis. *Biotechniques* **34**, 374–378.
- Sarafian, T. A. (1999). Methylmercury-induced generation of free radicals: biological implications. *Met. Ions Biol. Syst.* **36**, 415–444.
- Satarug, S., and Moore, M. R. (2004). Adverse health effects of chronic exposure to low-level cadmium in foodstuffs and cigarette smoke. *Environ. Health Perspect.* **112**, 1099–1103.

- Sharpless, N. E., Ramsey, M. R., Balasubramanian, P., Castrillon, D. H., and DePinho, R. A. (2004). The differential impact of p16(INK4a) or p19(ARF) deficiency on cell growth and tumorigenesis. *Oncogene* **23**, 379–385.
- Sherr, C. J., and Roberts, J. M. (1999). CDK inhibitors: positive and negative regulators of G1-phase progression. *Genes Dev.* **13**, 1501–1512.
- Sidhu, J. S., Hong, S., Erickson, A., Baker, A., Robinson, J., Vliet, P., and Faustman, E. M. (2003). Methyl mercury induces differential ubiquitin-conjugated protein levels in p53 variant mouse embryonal fibroblasts. *Toxicol. Sci.* **72**, 67.
- Sidhu, J. S., Ponce, R. A., Vredevogd, M. A., Yu, X., Gribble, E., Hong, S. W., Schneider, E., and Faustman, E. M. (2005). Cell cycle inhibition by sodium arsenite in primary embryonic rat midbrain neuroepithelial cells. *Toxicol. Sci.* **89**, 475–484.
- Song, E. J., Hong, H. M., and Yoo, Y. S. (2009). Proteasome inhibition induces neurite outgrowth through posttranslational modification of TrkA receptor. *Int. J. Biochem. Cell Biol.* **41**, 539–545.
- Stanhill, A., Haynes, C. M., Zhang, Y., Min, G., Steele, M. C., Kalinina, J., Martinez, E., Pickart, C. M., Kong, X. P., and Steele, D. (2006). An arsenite-inducible 19S regulatory particle-associated protein adapts proteasomes to proteotoxicity. *Mol. Cell.* **23**, 875–885.
- Steinman, H. A., Sluss, H. K., Sands, A. T., Pihan, G., and Jones, S. N. (2004). Absence of p21 partially rescues Mdm4 loss and uncovers an antiproliferative effect of Mdm4 on cell growth. *Oncogene* **23**, 303–306.
- Stewart, D., Killeen, E., Naquin, R., Alam, S., and Alam, J. (2003). Degradation of transcription factor Nrf2 via the ubiquitin-proteasome pathway and stabilization by cadmium. *J. Biol. Chem.* **278**, 2396–2402.
- Thompson, S. A., White, C. C., Krejsa, C. M., Eaton, D. L., and Kavanagh, T. J. (2000). Modulation of glutathione and glutamate-L-cysteine ligase by methylmercury during mouse development. *Toxicol. Sci.* **57**, 141–146.
- Tsirigotis, M., Zhang, M., Chiu, R. K., Wouters, B. G., and Gray, D. A. (2001). Sensitivity of mammalian cells expressing mutant ubiquitin to protein-damaging agents. *J. Biol. Chem.* **276**, 46073–46078.
- Tyers, M. (2004). Cell cycle goes global. *Curr. Opin. Cell Biol.* **16**, 602–613.
- Tyson, J. J., Csikasz-Nagy, A., and Novak, B. (2002). The dynamics of cell cycle regulation. *Bioessays* **24**, 1095–1109.
- Usami, H., Kusano, Y., Kumagai, T., Osada, S., Itoh, K., Kobayashi, A., Yamamoto, M., and Uchida, K. (2005). Selective induction of a tumor marker glutathione S-transferase P1 by proteasome inhibitors. *J. Biol. Chem.* **280**, 5267–5276.
- Uversky, V. N., Li, J., and Fink, A. L. (2001). Metal-triggered structural transformations, aggregation, and fibrillation of human alpha-synuclein. A possible molecular link between Parkinson's disease and heavy metal exposure. *J. Biol. Chem.* **276**, 44284–44296.
- Vabulas, R. M. (2007). Proteasome function and protein biosynthesis. *Curr. Opin. Clin. Nutr. Metab. Care* **10**, 24–31.
- Vaughan, J. R., Davis, M. B., and Wood, N. W. (2001). Genetics of Parkinsonism: a review. *Ann. Hum. Genet.* **65**, 111–126.
- Vengellur, A., Woods, B. G., Ryan, H. E., Johnson, R. S., and LaPres, J. J. (2003). Gene expression profiling of the hypoxia signaling pathway in hypoxia-inducible factor 1alpha null mouse embryonic fibroblasts. *Gene Expr.* **11**, 181–197.
- Verougstraete, V., Lison, D., and Hotz, P. (2003). Cadmium, lung and prostate cancer: a systematic review of recent epidemiological data. *J. Toxicol. Environ. Health B Crit. Rev.* **6**, 227–255.
- Vogel, D. G., Rabinovitch, P. S., and Mottet, N. K. (1986). Methylmercury effects on cell cycle kinetics. *Cell Tissue Kinet.* **19**, 227–242.
- Wagenknecht, B., Hermisson, M., Eitel, K., and Weller, M. (1999). Proteasome inhibitors induce p53/p21-independent apoptosis in human glioma cells. *Cell. Physiol. Biochem.* **9**, 117–125.
- Weiss, B., Clarkson, T. W., and Simon, W. (2002). Silent latency periods in methylmercury poisoning and in neurodegenerative disease. *Environ Health Perspect* **110**(Suppl. 5), 851–854.
- Wintermeyer, P., Kruger, R., Kuhn, W., Muller, T., Voitalla, D., Berg, D., Becker, G., Leroy, E., Polymeropoulos, M., Berger, K., et al. (2000). Mutation analysis and association studies of the UCHL1 gene in German Parkinson's disease patients. *Neuroreport* **11**, 2079–2082.
- Woods, J. S., and Ellis, M. E. (1995). Up-regulation of glutathione synthesis in rat kidney by methyl mercury. Relationship to mercury-induced oxidative stress. *Biochem. Pharmacol.* **50**, 1719–1724.
- Wright, G. W., and Simon, R. M. (2003). A random variance model for detection of differential gene expression in small microarray experiments. *Bioinformatics* **19**, 2448–2455.
- Wu, Q., Kirschmeier, P., Hockenberry, T., Yang, T. Y., Brassard, D. L., Wang, L., McClanahan, T., Black, S., Rizzi, G., Musco, M. L., et al. (2002). Transcriptional regulation during p21WAF1/CIP1-induced apoptosis in human ovarian cancer cells. *J. Biol. Chem.* **277**, 36329–36337.
- Yew, E. H., Cheung, N. S., Choy, M. S., Qi, R. Z., Lee, A. Y., Peng, Z. F., Melendez, A. J., Manikandan, J., Koay, E. S., Chiu, L. L., et al. (2005). Proteasome inhibition by lactacystin in primary neuronal cells induces both potentially neuroprotective and pro-apoptotic transcriptional responses: a microarray analysis. *J. Neurochem.* **94**, 943–956.
- Yu, X., Griffith, W. C., Hanspers, K., Dillman, J. F., III, Ong, H., Vredevogd, M. A., and Faustman, E. M. (2006). A system-based approach to interpret dose- and time-dependent microarray data: quantitative integration of gene ontology analysis for risk assessment. *Toxicol. Sci.* **92**, 560–577.
- Yu, X., Hong, S., and Faustman, E. M. (2008a). Cadmium-induced activation of stress signaling pathways, disruption of ubiquitin-dependent protein degradation and apoptosis in primary rat Sertoli cell-gonocyte cocultures. *Toxicol. Sci.* **104**, 385–396.
- Yu, X., Hong, S., Moreira, E. G., and Faustman, E. M. (2009). Improving in vitro Sertoli cell/gonocyte co-culture model for assessing male reproductive toxicity: lessons learned from comparisons of cytotoxicity versus genomic responses to phthalates. *Toxicol. Appl. Pharmacol.* **239**, 325–336.
- Yu, X., Robinson, J. F., Gribble, E., Hong, S. W., Sidhu, J. S., and Faustman, E. M. (2008b). Gene expression profiling analysis reveals arsenic-induced cell cycle arrest and apoptosis in p53-proficient and p53-deficient cells through differential gene pathways. *Toxicol. Appl. Pharmacol.* **233**, 389–403.
- Yu, X., Sidhu, J. S., Hong, S., and Faustman, E. M. (2005). Essential role of extracellular matrix (ECM) overlay in establishing the functional integrity of primary neonatal rat Sertoli cell/gonocyte co-cultures: an improved in vitro model for assessment of male reproductive toxicity. *Toxicol. Sci.* **84**, 378–393.
- Zhang, W., Tong, Q., Li, S., Wang, X., and Wang, Q. (2008). MG-132 inhibits telomerase activity, induces apoptosis and G(1) arrest associated with upregulated p27kip1 expression and downregulated survivin expression in gastric carcinoma cells. *Cancer Invest.* **26**, 1032–1036.
- Zimmermann, J., Erdmann, D., Lalande, I., Grossenbacher, R., Noorani, M., and Furst, P. (2000). Proteasome inhibitor induced gene expression profiles reveal overexpression of transcriptional regulators ATF3, GADD153 and MAD1. *Oncogene* **19**, 2913–2920.